

中山醫學大學醫學研究所博士論文

Ph. D. Thesis, Institute of Medicine,

Chung Shan Medical University

小腦脊髓運動失調症的分子診斷及其第三
型和第七型致病機轉之研究

Molecular diagnosis of spinocerebellar ataxias and
studies of pathogenesis of spinocerebellar ataxia
type 3 and type 7

指導教授：謝明麗 教授 Mingli Hsieh, Ph.D.

李 娟 教授 Chuan Li, Ph.D.

研究生：蔡蕙芳 Hui-Fang Tsai

中華民國九十四年一月

January, 2005

中文摘要

人類小腦脊髓運動失調症候群是一種「體染色體顯性的遺傳性疾病」。造成此疾病的原因是由一段不穩定的 CAG 三核酸重覆序列倍增突變(amplification mutation)，轉譯出的多穀醯胺酸突變蛋白(polyglutamine)所形成。這些小腦脊髓運動失調症候群的遺傳疾病有一個明顯的特徵就是遺傳的期望值，它可以傳給子代且發病年齡越早漸進性神經退化越嚴重。目前我們的實驗室已鑑定 7 種疾病包括 spinocerebellar ataxia type 1 (SCA1), SCA2, SCA3/Machado-Joseph disease (MJD), SCA6, SCA7, SCA8, SCA12 除了 SCA8 和 SCA12 外，它們大都屬於 CAG 三核酸重覆序列倍增突變(trinucleotides repeat expansion)。從我們實驗室收集的病人檢體中利用 PCR 的檢測方法，一共分析 211 個體染色體顯性遺傳的病人，其中有 202 個病人來自 81 個體染色體顯性遺傳的家族而另外 9 個為偶發性的病人，其結果顯示在台灣 SCA3/ MJD 這型的病人佔最多，它約佔 32% (26 個家族)，其次為 SCA2 (11%，9 個家族)，SCA1 和 SCA7 佔最少(1.2%，1 個家族)。此外，我們是台灣第一個在產前診斷中成功的鑑定出胎兒具有 MJD 的突變基因，利用胎兒的羊水 DNA 鑑定其在 MJD 的基因座上有 74 個 CAG 核酸重覆序列倍增，並且從引產中取得胎兒的纖維母細胞，並鑑定出在胎兒早期即有此種突變的 ataxin-3 蛋白。另一方面我們想要了解 MJD 和細胞凋亡路徑的關係，實驗中利用不同促使細胞凋亡的誘導劑如 tunicamycin， brefeldin A (ER stress) 和 staurosporine (non-ER stress)，結果顯示出突變的 ataxin-3 蛋白在扮演細胞凋亡的角色中是走 non-ER stress 路徑，有趣的是我們發現到在未做任何處的條件下，在西方點墨法和免疫細胞化學組織染色法中發現含突變的 ataxin-3 的細胞株其 Bcl-2 蛋白表現量下降，且細胞質內的 cytochrome c 蛋白表現量增加。同樣 Bcl-2 蛋白表現量下降也在 MJD 胎兒的纖維母細胞中發現。另外，這種多穀醯胺酸突變蛋白所造成疾病常和不正常的蛋白聚集堆積有關係，而 molecular chaperones 對於此種漸進性神經退化疾病扮演著重要的角色。所以我們取得了兩個 SCA7 病人的淋巴母細胞株各包括 100 個和 41 個 CAG 核酸重覆序列，用來研究多穀醯胺酸擴增對於熱休克蛋白是否會有影響。在西方點墨法和免疫細胞化學組織染色法中發現病人的淋巴母細胞株內的 Hsp27 和 Hsp70 蛋白表現量明顯下降(和正常人的淋巴母細胞株作比較)，然而，我們的結果雖顯示 Hsp27 和 Hsp70 蛋白在 SCA7 病人的淋巴母細胞株是有缺陷，但它們對於熱休克的刺激卻有正常的反應。這結果推測出突變的 ataxin-7 造成細胞內的 Hsp27 和 Hsp70 蛋白減少，可能會引起結構摺疊異常的蛋白堆積和細胞毒性的壓力。綜合以上的研究，我們的結果顯示出含有多穀醯胺酸的突變蛋白會使抗細胞凋亡的蛋白如 Bcl-2 和 Hsp27 及 molecular chaperones Hsp70 的蛋白表現降低，這在研究多穀醯胺酸的突變蛋白和細胞凋亡過程的探討或許扮演著重要的角色。

Abstract

The spinocerebellar ataxias (SCAs) are inherited autosomal dominant diseases. An expanded CAG repeat within the disease gene encodes a polyQ repeat in the mutant proteins. Compelling features of SCAs are the genetic anticipation with an earlier age at onset and a more severe progression of disease in successive generations. Seven different loci causing spinocerebellar ataxia (SCA) have been studied in our laboratory, including SCA1, SCA2, SCA3/MJD (Machado-Joseph disease), SCA6, SCA7, SCA8 and SCA12 loci. Most of these diseases (except SCA8 and SCA12) are caused by CAG trinucleotide expansion in the coding region of the respective gene. To determine the relative contributions of known ataxia genes in the patient population sent to our laboratory, we genetically evaluated 202 patients with dominantly inherited ataxia from 81 families and 9 patients with sporadic ataxia by the use of radioactive genomic polymerase chain reaction (PCR). Our results showed that SCA3/MJD was the most common genotype in our collection, accounting for 32% of cases (26 families). SCA2 was the second frequent genotype (11%, 9 families), SCA1 and SCA7 were much less frequent (1.2%, 1 family for each genotype). Furthermore, the first case of MJD prenatal diagnosis in Taiwan was successfully performed in our laboratory. We identified the presence of a 74 CAG expansions on MJD gene from the amniocentesis sampling by the prenatal diagnosis. MJD fibroblast cells were obtained from the aborted fetus after termination of pregnancy. The expression of mutant ataxin-3 was also identified in the fetal fibroblast cells. On the other hand, we are interested in the apoptotic pathway involved in the MJD. The results from cells treated with different apoptosis inducers, including tunicamycin, brefeldin A (ER stress) and STS (non-ER stress), indicated that mutant ataxin-3 plays role(s) in the non-ER stress induced apoptosis. Interestingly, under basal conditions, Western blot and immunocytochemical analysis showed a significant decrease of Bcl-2 protein expression and an increase of cytochrome c in cells containing expanded ataxin-3 when compared with those of the parental cells. The same reduction of Bcl-2 was further confirmed in fibroblast cells with mutant ataxin-3. In addition, because the polyglutamine disease is associated with abnormal protein aggregation, the molecular chaperones may play a role in disease progression. Two SCA7 lymphoblastoid cell lines with 100 and 41 polyglutamine repeats were utilized to examine the effects of polyglutamine expansion on heat shock proteins. A significant decrease of Hsp 27 and Hsp70 protein expression was observed through Western blot and immunocytochemical analysis. However, our results showed that even though the protein expression of Hsp27 and Hsp70 is defective, a normal heat shock response is present in lymphoblastoid cells expressing mutant ataxin-7. The

results suggested that the reduction of Hsp 27 and Hsp70 proteins in the presence of mutant ataxin-7 might lead to misfolded protein accumulation and cell-toxicity stress. Taken together, our results indicated that the reduction of the anti-apoptotic proteins, Bcl-2 and Hsp27, and molecular chaperones, Hsp70, in the presence of polyglutamine proteins may contribute together to the cell apoptotic process.

Table of contents

Chinese abstract-----	I
English abstract-----	II
Chapter 1: Analysis of trinucleotide repeats in different SCA loci in spinocerebellar ataxia patients and in normal population of Taiwan	
Abstract-----	1
1-1 Introduction-----	3
1-2 Materials and Methods-----	5
1-3 Results-----	7
1-4 Discussion-----	10
1-5 References-----	17
Chapter 2: Prenatal diagnosis of Machado-Joseph disease/ Spinocerebellar Ataxia Type 3 in Taiwan: early detection of expanded ataxin-3	
Abstract-----	23
2-1 Introduction-----	24
2-2 Materials and Methods-----	27
2-3 Results-----	30
2-4 Discussion-----	32
2-5 References-----	38

Chapter 3: Full-Length Expanded Ataxin-3 Enhances Mitochondrial-Mediated Cell Death and Decreases Bcl-2 Expression in Human Neuroblastoma Cells

Abstract-----	42
3-1 Introduction-----	44
3-2 Materials and Methods-----	47
3-3 Results-----	52
3-4 Discussion-----	57
3-5 References-----	75

Chapter 4: Decreased expression of Hsp 27 and Hsp70 in transformed lymphoblastoid from patients with Spinocerebellar ataxia type 7 (SCA7)

Abstract-----	80
4-1 Introduction-----	82
4-2 Materials and Methods-----	86
4-3 Results-----	92
4-4 Discussion-----	98
4-5 Reference-----	114
Appendix-----	122

Chapter 1: Analysis of trinucleotide repeats in different SCA loci in spinocerebellar ataxia patients and in normal population of Taiwan

ABSTRACT

To identify various subtypes of spinocerebellar ataxias (SCAs) among autosomal dominant cerebellar ataxia (ADCA) patients referred to our research center, SCA1, SCA2, SCA3/MJD (Machado-Joseph disease), SCA6, SCA7, SCA8 and SCA12 loci were assessed for expansion of trinucleotide repeats. A total of 211 ADCA patients, including 202 patients with dominantly inherited ataxia from 81 Taiwanese families and nine sporadic cases, were included in this study and subjected to polymerase chain reaction (PCR) analysis. The amplified products of all loci were analyzed on both 3% agarose gels and 6% denaturing urea-polyacrylamide gels. PCR-based Southern blots were also applied for the detection of SCA7 locus. The SCA1 mutation was detected in six affected individuals from one family (1.2%) with expanded alleles of 50-53 CAG repeats. Fourteen individuals from nine families (11%) had a CAG trinucleotide repeat expansion at the SCA2 locus, while affected SCA2 alleles have 34-49 CAG repeats. The SCA3/MJD CAG trinucleotide repeat expansion in 60 affected individuals from 26 families (32%) was expanded to 71-85 CAG repeats. As for the SCA7 locus, there were two affected individuals from one family (1.2%)

possessed 41 and 100 CAG repeats, respectively. However, we did not detect expansion in the SCA6, SCA8 and SCA12 loci in any patient. The SCA3/MJD CAG expansion was the most frequent mutation among the SCA patients. The relative prevalence of SCA3/MJD in Taiwan was higher than that of SCA2, SCA1 and SCA7.

1-1 INTRODUCTION

Autosomal dominant cerebellar ataxias (ADCAs) are a clinically and genetically heterogeneous group of neurodegenerative disorders displaying clinical characteristics of progressive degeneration in the cerebellum, spinal cord, and extrapyramidal (1). Clinically, most patients could be classified into ADCA type I - III, based on the Harding Scheme. However, in a classification system based on molecular analysis, the genetic etiologies of at least 20% of the ADCAs have not yet been determined (2). To date, at least 13 different loci causing SCAs have been genetically mapped, including the spinocerebellar ataxia type 1 (SCA1) on chromosome 6p (3), SCA2 on 12q (4-6), SCA3/Machado-Joseph disease (MJD) on 14q (7-8), SCA4 on 16q (9), SCA5 on 11cen (10), SCA6 on 19p (11), SCA7 on 3p (12), SCA8 on 13q (13), SCA10 on 22q (14-15), SCA11 on 15q (16), SCA12 on 5q (17), SCA17/TBP on 6q (18) and dentatorubro-pallidoluyasian atrophy (DRPLA) on 12p (19, 20). The mutations causing 10 of these diseases, including SCA1, SCA2, SCA3, SCA6, SCA7, SCA8, SCA10, SCA12, SCA17, and DRPLA, have been identified. All these SCAs (except SCA8, SCA10 and SCA12) are caused by a CAG trinucleotide repeat expansion in the coding region of the respective genes, resulting in an expanded glutamine repeat, whereas SCA8, SCA10 and SCA12 are caused by untranslated (CTA)_n/(CTG)_n, (ATTCT)_n and (CAG)_n expansions (13-15,17), respectively. Typical onset of SCA symptoms usually occurs between the ages of 30 and 40 years, and symptoms are slowly progressed. The expanded repeats are unstable between generations and this intergenerational instability gives rise to an unusual pattern of inheritance-anticipation, which means decreasing age at onset of symptoms and increasing disease severity in successive generations (21). The phenomenon of

genetic anticipation is based on the expansion of trinucleotide repeats with an unstable intergenerational transmission. However, the molecular mechanisms of genomic instabilities are still unknown.

SCA subtypes among ADCA patients vary highly in different ethnic populations. In this study, we analyzed the CAG repeats at the SCA1, SCA2, SCA3/MJD, SCA6, SCA7, SCA8 and SCA12 loci in 81 Taiwanese families with SCA or late-onset cerebellar ataxia to determine the SCAs subtypes of these individuals and the results have identified SCA1 in six affected individuals, SCA2 in 14 (22), SCA3/MJD in 60 (23), and SCA7 in two (24). The CAG repeat distributions at the SCA1, SCA2, SCA3/MJD, SCA6, SCA7, SCA8 and SCA12 loci in Taiwanese normal population were also determined.

1-2 MATERIALS AND METHODS

SUBJECTS

A total of 202 patients with dominantly inherited ataxia from 81 Taiwanese families and nine patients with sporadic ataxias were analyzed. The diagnosis of SCA was determined by clinical examination by an experienced neurologist based on established diagnostic criteria (25). Inclusion criteria of SCA were progressive, adult cerebellar ataxia in a pure form, and in association with at least one of the following signs: ophthalmoplegia, optic atrophy, pyramidal signs, decreased vibration and/or tactile and/or pain sensation, dementia, and extrapyramidal signs. The age at presentation of these diseases varied from 7 to 79 years. These patients were unrelated to one another at least to the second cousin level. Family history and blood samples were collected, with an appropriate consent, from each patient. None of the patients referred with SCA to the genetic center and fulfilling criteria for the disorder was excluded from the investigation. As control subjects, blood samples of unrelated healthy Taiwanese individuals from National Blood Center and Chung Shan Genetic Center (from 17 to 65 years old) were analyzed under an unselected basis.

DNA EXTRACTION AND PCR AMPLIFICATION

DNA samples were purified from peripheral blood lymphocytes using a standard protocol (26). SCA1 loci were amplified by using primers Rep1 and Rep2 under the conditions described by Orr et al. (3). SCA2, SCA3, SCA6, SCA7, SCA8 and SCA12 loci were amplified by using primers SCA2-A and SCA2-B, MJD52 and MJD25a, S-5-F1 and S-5-R1, 4U1024 and 4U716, SCA8-F3 and SCA8-R4,

SCA12-A and SCA12-B, respectively (5, 7, 11-13, 17). Polymerase chain reaction (PCR) was performed in a final volume of 20 μ l containing 50 ng of genomic DNA, 10 mM Tris-HCl (pH8.8), 1.5 mM $MgCl_2$, 50 mM KCL, 0.1% Triton X-100, 10% dimethylsulfoxide, 250 μ M each dCTP, dGTP, and dTTP, 25 μ M dATP, 1.5 μ Ci³⁵S-alpha-dATP125 ng of appropriate primers and 3 units of Taq DNA polymerase as previously reported (5, 7, 11-13, 17). To determine the exact number of CAG repeats, the PCR products were analyzed on denaturing 6% polyacrylamide gels in parallel with a pGEM sequencing ladder. In the case of patients, the amplified products of all loci were checked on 3% agarose gels and then run on 6% denaturing urea-polyacrylamide gels along with positive controls and allelic markers of known sizes. For determination of repeat numbers at the SCA7 loci, PCR-based southern blot was performed to confirm the presence of mutations as previously described (24).

1-3 RESULTS

Frequency analysis of SCA1, SCA2, SCA3/MJD, SCA6, SCA7, SCA8 and SCA12 expanded alleles in SCA patients

To estimate the relative distribution of each identified SCA gene in clinical ataxia cases, patients who were initially negative in specific ataxia gene testing (SCA3) were analyzed further for a panel of ataxia genes including SCA1, SCA2, SCA6, SCA7, SCA8 and SCA12.

At the SCA1 locus, six affected individuals were identified from one family. Expanded alleles ranging from 50 to 53 repeats were found in three patients (with an age of presentation between 33 and 40) and three asymptomatic carriers (at the ages of 11-20). In addition, 14 individuals (13 patients and one asymptomatic individual) from nine families had a CAG repeat expansion at the SCA2 locus. It was noted that the normal SCA2 alleles contained 22 or 24 triplets, while the expanded allele size ranged from 34 to 49.

Moderate expansions of CAG repeat at the SCA3/MJD1 locus were found in 60 individuals from 26 families that had ataxia with a dominant inheritance. The expanded alleles ranged from 71 to 85 repeat units, with 80 repeats being the most frequent. In paternal transmissions, the average increase was three repeats, while in maternal transmissions, the average was a 0.2 repeat increase. These results supported the suggestion that paternal transmissions were less stable than maternal ones.

A 41 CAG repeat expansion at the SCA7 locus was firstly detected in one proband's asymptomatic father (24). A remarkable instability of the CAG repeat number during transmission from father to son (41 vs. 100) was observed in the SCA7 family. Clinical anticipation was significant in this family including an infantile case, who was found to have nystagmus from the age of 1 month (24).

A summary of the results was presented in Table 1. The numbers of unrelated families with positive test results were one for SCA1, nine for SCA2, 26 for SCA3/MJD, and one for SCA7. However, no patient was detected with expansion in the SCA6, SCA8 and SCA12 loci. The prevalence of SCA3 in the 81 unrelated families with autosomal dominant was the highest as 32% (n=26), followed by SCA2 (11%, n=9), SCA1 (1.2%, n=1) and SCA7 (1.2%, n=1) (Table1). Table 2 summarized the common manifestations of patients with different subtypes of SCAs. In addition, distribution of the genetically defined ADCAs in Taiwanese was compared with those of other areas in the world (Table 3). It was noted that the relative prevalence of SCA3/MJD in this study was significantly higher than those of Korean and Australian, but was similar to that of Chinese origin, as shown in Table 3.

The distribution of CAG/CTG repeats at SCA1, SCA2, SCA3/MJD, SCA6, SCA7, SCA8 and SCA12 loci in Taiwanese population

Evidence from several populations has suggested that the disease prevalence of various SCAs may be associated with the presence of large normal alleles at the respective loci. The numbers of trinucleotide repeat in different SCA genes of healthy controls randomly selected from a large collection (see Materials and Methods) were

analyzed and the results are summarized in Table 4. The normal range of SCA1 locus was from 22 to 32 repeats, with the more common being around 30 repeats (32%). In SCA2, the normal range was from 16 to 30 repeat units as assessed 114 normal controls. Unlike SCA1 or SCA3/MJD, the size distribution of the normal SCA2 alleles was less polymorphous, with the allele of 22 repeats accounting for about 91%. Homozygosity was detected in 80.7% normal individuals. At the SCA3/MJD1 locus, the CAG repeat length in 258 normal alleles ranged from 13 to 44, with a mean of 24 repeats.

The distribution of the CAG repeats of SCA6 gene in 138 normal controls ranged from 6 to 16 repeats, with the more common being around 12-13 repeats. At the SCA7 locus, the distribution of the CAG repeats in 100 normal chromosomes ranged from six to 17 repeats, with the more common being around 8-13 repeats.

Homozygosity of SCA7 was identified in 74% of our population. Analysis of the SCA8 locus was conducted for 100 normal chromosomes, with the size ranging from 17 to 46 repeats. More than 99% of these alleles had 18-33 combined repeats. At the SCA12 locus, the CAG repeats in 108 normal chromosomes ranged from seven to 25. The more common alleles were around 10-17 repeats, with the most frequent allele being with 10 repeat (20%) units.

1-4 DISCUSSION

The clinical classification of the ADCAs has been difficult due to the overlap in clinical signs. This study was to estimate the frequency for each mutation in the SCAs for which routine genetic testing is currently convenient. Our results showed that, among the 81 families studied, the SCA1 mutation was detected in one family (1.2%), SCA2 in nine families (11%), SCA3/MJD in 26 families (32%), and SCA7 in one family (1.2%). We could not detect any mutation in the remaining 44 families (54%). From our analysis, the relative prevalence of the families with SCA3 mutation was the highest. Such high frequency of SCA3 in the 81 ADCA families may be relevant to the immigrants from Mainland Chinese (27). Second to SCA3/MJD, SCA2 was a common dominantly inherited cerebellar ataxia in our analysis, as it was in Mainland Chinese (27). The relative frequencies of trinucleotide repeat diseases varied among different ethnic groups in the world (Table 3). However, the mutations of 44 families with positive family history of the ADCAs remain unidentified, suggesting the existence of other disease loci.

However, the SCA6 mutations were not found in our patients, who reside mostly in the central and southern areas of Taiwan Island. It came to our attention that recently Soong et al. reported a geographic cluster of families with SCA6 on Taiwan, with 19.8% of healthy individuals having more than 13 CAG repeats (28). Thus, we compared the CAG repeats of SCA6 in the normal controls of the present study to other studies. The observation also provided evidence of a greater frequency with CAG repeats larger than 13 in our healthy control population (15%), similar to that in Japanese population (20%), than that reported in Caucasian population (4%).

However, the reasons for differences of the prevalence of SCA6 in Taiwanese populations from other geographic areas are not clear, but may be explained by a founder effect, as suggested by Soong et al (28). It was reported that the majority of SCA6 patients in Taiwan (70%) shared the same genotypes in addition to the geographic clustering of the SCA6 families (28). Therefore, a regional difference in the frequency of SCA6 in Taiwan is possible. Without a thorough population survey, caution should be exercised when it comes to the interpretation of the disease frequency.

It was reported that the normal range for SCA8 alleles was 16-91 combined CTA/CTG triplet repeats, with more than 99% of these alleles being 16-37 repeats and the patients with SCA8 mutation carry expanded alleles with 107-127 pure CTGs (13). Recently, Elena et al. (2001) reported that the CTA/CTG repeats in the SCA8 locus varied from 15 to 75 triplets among normal individuals (29). We found here a distribution of normal alleles ranged from 17 to 46 repeats with 99% of these alleles being 18-33 combined repeats. The most frequent allele contained 28 repeats, accounting for 16% of all normal controls analyzed. The distribution of normal alleles in this study was similar to that previously reported in other ethnic groups (13, 29). However, no SCA8 mutation was identified in our patient collection.

Recently, Holmes and colleagues reported a novel form of ADCA, named SCA12 (17). The disease was associated with an expanded CAG repeat in the 5' untranslated region of the gene PPP2R2B, encoding a brain-specific regulatory subunit of protein phosphatase PP2A. Normal CAG lengths in the SCA12 gene ranged from seven to 28 repeats, whereas expanded alleles contained 66 to 78

repeats (17). In our study, normal repeats ranged from seven to 25 repeats, with the most frequent allele containing 10 repeats (20%). It was noted that the number of large alleles with more than 15 triplets was significantly greater in our population than in the Indian and the French control subjects (30). However, no SCA12 allele with more than 25 CAG repeats was found among the 108 normal chromosomes. As an association between prevalence of SCAs and frequency of large normal CAG repeat sizes has been found in Japanese and Caucasian populations, it was speculated that these may contribute to the generation of mutated alleles in the dominantly inherited SCAs (31). We speculated that it is the upper tails of the large normal allele stochastically undergo an expansion mutation to produce the new expanded alleles. However, this speculation remained to be confirmed. This is the first report for the distribution of the CAG repeats of SCA12 gene in normal populations in Taiwan. Although we have not detected any expanded alleles in our database, these results together with findings in other populations indicated that the SCA12 mutation may be a rare cause of cerebellar ataxia worldwide (32- 34).

Table 1: Summary of the distribution of expanded trinucleotide repeats in various SCA loci among 81 clinically diagnosed ADCA families in Taiwan

Type	Affected Pedigree alleles	Pedigree No.	Frequency (%)	Range of expanded repeat numbers
SCA1	6	1	1.2 %	50-53
SCA2	14	9	11 %	34-49
SCA3/MJD	60	26	32 %	71-85
SCA6	0	0	0 %	-----
SCA7	2	1	1.2 %	41-100
SCA8	0	0	0 %	-----
SCA12	0	0	0 %	-----
Total	82	37		

Table 2: Comparison of clinical manifestations of patients with different subtypes of SCAs

	SCA1	SCA2	SCA3/MJD	SCA7
No. of patients/No. of kindreds	3/1	13/9	43/26	1/1
Clinical manifestation, No.				
Ataxia	3	13	43	1
Swallowing difficulties	2	4	26	1
Nystagmus	0	4	28	1
Slow saccades	2	11	14	1
Ophthalmoplegia	2	4	29	1
Facial and lingual fasciculation	0	3	33	0
Bulging eyes	0	0	13	0
Spasticity	3	0	24	0
Hyperreflexia	3	0	37	0
Hyporeflexia	0	9	0	1
Babinski signs	2	3	28	0
Amyotrophy	0	4	17	1
Chorea	0	1	2	0
Dementia	0	4	14	1

Table 3: Frequency distribution of Spinocerebellar Ataxia subtypes in different ethnic populations

Ethnicity	Total No. Families	Frequency (%)							Year of publication
		SCA1	SCA2	SCA3	SCA6	SCA7	SCA8	SCA12	
White (31)	177	15	14	30	5	NT*	NT	NT	1998
Japanese (31)	202	3	5	43	11	NT	NT	NT	1998
Portuguese(35)	48	0	4	74	0	NT	NT	NT	1998
Mainland Chinese (27)	85	5	6	48	0	0	NT	NT	2000
Australian (36)	88	16	6	12	17	2	NT	NT	2000
Korean (37)	NA	3.9	14.5	15.8	2.6	2.6	NT	NT	2001
Taiwanese	81	1.2	11	32	0	1.2	0	0	Present study

* NT: Not Test

Table 4: Summary of the distribution of CAG/CTG repeat numbers of the SCAs in normal population in Taiwan

Type	Allele range (in repeats)	Total No. of alleles	Observed heterozygosity(%)	Allele with maximum frequency (in repeats)
SCA1	22-32	158	86 %	30
SCA2	16-30	114	19.3 %	22
SCA3/MJD	13-44	258	93 %	16
SCA6	6-16	138	94.2 %	13
SCA7	6-17	100	26 %	12
SCA8	17-46	100	99 %	28
SCA12	7-25	108	81.4 %	10

1-5 REFERENCES

1. Harding AE. The clinical features and classification of the late onset autosomal dominant cerebellar ataxias: a study of 11 families, including descendants of the Drew family of Walworth. *Brain* 1982; 105: 1-28.
2. Schols L, Amoiridis G, Buttner T, Przuntek H, Eppelen JT, Riess O. Autosomal dominant cerebellar ataxia: phenotypic differences in genetically defined subtypes? *Ann Neurol* 1997; 42: 924-932.
3. Orr HT, Chung M, Banfi S et al. Expansion of an unstable trinucleotide CAG repeat in spinocerebellar ataxia type 1. *Nat Genet* 1993; 4: 221-226.
4. Imbert G, Saudou F, Yvert G et al. Cloning of the gene for spinocerebellar ataxia 2 reveals a locus with high sensitivity to expanded CAG/glutamine repeats. *Nat Genet* 1996; 14: 285-291.
5. Pulst SM, Nechiporuk A, Nechiporuk T et al. Moderate expansion of a normally biallelic trinucleotide repeat in spinocerebellar ataxia type 2. *Nat Genet* 1996; 14: 269-276.
6. Sanpei K, Takano H, Igarashi S et al. Identification of the spinocerebellar ataxia type 2 gene using a direct identification of repeat expansion and cloning technique, DIRECT. *Nat Genet* 1996; 14: 277-284.
7. Kawaguchi Y, Okamoto T, Taniwaki M et al. CAG expansions in a novel gene

from Machado-Joseph disease at chromosome 14q32.1. Nat Genet 1994: 8: 221-228.

8. Takiyama Y, Nishizawa M, Tanaka H et al. The gene for Machado-Joseph disease maps to human chromosome 14q. Nat Genet 1993: 4: 300-303.

9. Flanigan K, Gardner K, Alderson K et al. Autosomal dominant spinocerebellar ataxia with sensory axonal neuropathy (SCA4): clinical description and genetic localization to chromosome 16q22.1 Am J Hum Genet 1996: 59: 392-399.

10. Ranum LP, Schut LJ, Lundgren JK, Orr HT, Livingston DM. Spinocerebellar ataxia type 5 in a family descended from the grandparents of President Lincoln maps to chromosome 11. Nat Genet 1994: 8: 280-284.

11. Zhuchenko O, Bailey J, Bonnen P et al. Autosomal dominant cerebellar ataxia (SCA6) associated with small polyglutamine expansions in the alpha 1A-voltage-dependent calcium channel. Nat Genet 1997: 15: 62-69.

12. David G, Abbas N, Stevanin G et al. Cloning of the SCA7 gene reveals a highly unstable CAG repeat expansion. Nat Genet 1997: 17: 65-70.

13. Koob MD, Moseley ML, Schut LJ, Benzow KA, Bird TD, Day JW, Ranum LP. An untranslated CTG expansion causes a novel form of spinocerebellar ataxia (SCA8). Nat Genet 1999: 21: 379-384.

14. Matsuura T, Yamagata T, Burgess DL et al. Large expansion of the ATTCT pentanucleotide repeat in spinocerebellar ataxia type 10. Nat Genet 2000: 26:

191-194.

15. Zu L, Figueroa KP, Grewal R, Pulst SM. Mapping of a new autosomal dominant spinocerebellar ataxia to chromosome 22. *Am J Hum Genet* 1999; 64: 594-599.

16. Worth PF, Giunti P, Gardner-Thorpe C, Dixon PH, Davis MB, Wood NW. Autosomal dominant cerebellar ataxia type III: linkage in a large British family to a 7.6-cM region on chromosome 15q14-21.3. *Am J Hum Genet* 1999; 65: 420-426.

17. Holmes SE, O'Hearn EE, McInnis MG et al. Expansion of a novel CAG trinucleotide repeat in the 5' region of PPP2R2B is associated with SCA12. *Nat Genet* 1999; 23: 391-392.

18. Nakamura K, Jeong SY, Uchihara T et al. SCA17, a novel autosomal dominant cerebellar ataxia caused by an expanded polyglutamine in TATA-binding protein. *Hum Mol Genet* 2001; 10: 1441-1448.

19. Koide R, Ikeuchi T, Onodera O et al. Unstable expansion of CAG repeat in hereditary dentatorubral-pallidoluysian atrophy (DRPLA). *Nat Genet* 1994; 6: 9-13.

20. Nagafuchi S, Yanagisawa H, Sato K et al. Dentatorubral and pallidoluysian atrophy expansion of an unstable CAG trinucleotide on chromosome 12p. *Nat Genet* 1994; 6: 14-18.

21. Sutherland GR, Richards RI. Simple tandem repeats and human genetic disease. *Proc Natl Acad Sci USA* 1995; 92: 3636-3641.

22. Hsieh M, Li SY, Tsai CJ et al. Identification of five spinocerebellar ataxia type 2 pedigrees in patients with autosomal dominant cerebellar ataxia in Taiwan. *Acta Neurol Scand* 1999; 100: 189-194.
23. Hsieh M, Tsai HF, Lu TM, Yang CY, Wu HM, Li SY. Studies of the CAG repeat in the Machado-Joseph disease gene in Taiwan. *Hum Genet* 1997; 100: 155-162.
24. Hsieh M, Lin SJ, Chen JF et al. Identification of spinocerebellar ataxia type 7 mutation in Taiwan: application of PCR –based Southern blot. *J Neurol* 2000; 247: 623-629.
25. Harding AE. Clinical features and classification of inherited ataxias. *Adv Neurol* 1993; 61: 1-14.
26. Sambrook, J, Fritsch EF, Maniatis T. *Molecular cloning. A laboratory manual*. 2nd ed. Cold Spring Harbor Laboratory Press, USA. 1989.
27. Tang B, Liu C, Shen L et al. Frequency of SCA1, SCA2, SCA3/MJD, SCA6, SCA7 and DRPLA CAG trinucleotide repeat expansion in patients with hereditary spinocerebellar ataxia from Chinese Kindreds. *Arch Neurol* 2000; 57: 540-544.
28. Soong BW, Lu YC, Choo KB, Lee HY. Frequency analysis autosomal dominant cerebellar ataxia in Taiwanese patients and clinical and molecular characterization of spinocerebellar ataxia type 6. *Arch Neurol* 2001; 58: 1105-1109
29. Cellini E, Nacmias B, Forleo P et al. Genetic and clinical analysis of

- spinocerebellar ataxia type 8 repeat expansion in Italy. Arch Neurol 2001: 58: 1856-1860.
30. Fujigasaki H, Verma IC, Camuzat A et al. SCA12 is a rare locus for autosomal dominant cerebellar ataxia: a study of an Indian family. Ann Neurol 2001: 49: 117-121.
31. Takano H, Cancel G, Ikeuchi T et al. Close associations between prevalences of dominantly inherited spinocerebellar ataxias with CAG-repeat expansions and frequencies of large normal CAG alleles in Japanese and Caucasian populations. Am J Hum Genet 1998: 63: 1060-1066.
32. Cholfin JA, Sobrido MJ, Perlman S, Pulst SM, Geschwind DH. The SCA12 mutation as a rare cause of spinocerebellar ataxia. Arch Neurol 2001: 58: 1833-1835.
33. Subramony SH, Filla A. Autosomal dominant spinocerebellar ataxias ad infinitum? Neurology 2001: 56: 287-289.
34. Worth PF, Wood NW. Spinocerebellar ataxia type 12 is rare in the United Kingdom. Neurology. 2001: 56: 419-420.
35. Silveria I, Coutinho P, Maciel P et al. Analysis of SCA1, DRPLA, MJD, SCA2, and SCA6 CAG repeats in 48 Portuguese ataxia families. Am J Med Genet 1998: 81: 134-138.
36. Storey E, du Sart D, Shaw JH et al. Frequency of spinocerebellar ataxia types 1, 2,

3, 6, and 7 in Australian patients with spinocerebellar ataxia. *Am J Med Genet* 2000; Dec 11; 95(4): 351-7.

37. Kim JY, Park SS, Joo SI, Kim JM, Jeon BS. Molecular analysis of Spinocerebellar ataxia in Koreans: frequencies and reference ranges of SCA1, SCA2, SCA3, SCA6, and SCA7. *Mol Cells* Dec 2001; 31; 12(3): 336-41.

Chapter 2: Prenatal diagnosis of Machado-Joseph disease/ Spinocerebellar Ataxia Type 3 in Taiwan: early detection of expanded ataxin-3

ABSTRACT

Machado-Joseph disease (MJD)/Spinocerebellar Ataxia Type 3 (SCA3) is a rare autosomal dominative disorder in which one of the neurodegenerative disorders caused by a translated CAG repeat expansion. Here, we present the first prenatal diagnosis of MJD in Taiwan by polymerase chain reaction (PCR) in a woman whose husband was known to carry an unstable CAG repeat expansion in the MJD gene. After evaluation of motivation and psychological tolerance, the amniocentesis was performed at the 13 weeks' gestation. The diagnosis was made using a simple non-radioactive PCR for rapid detection of the presence of an expanded MJD allele. Meanwhile, by the use of radioactive PCR, we identified the presence of an unusual shortness of CAG expansion in MJD gene with 74 repeats in fetus compared with 78 repeats in the father. After termination of pregnancy, Western blot analysis further confirmed the presence of the normal and mutant ataxin-3 in the fetal tissue. In summary, we have performed the first prenatal diagnosis of MJD in Taiwan, and described our experience with at-risk male requesting counseling, carrier testing and prenatal diagnosis for Machado-Joseph disease. Early detection of both normal and expanded ataxin-3 in fetal tissues was first demonstrated in the present study.

2-1 INTRODUCTION

Machado-Joseph disease (MJD) belonging to the autosomal dominant cerebellar ataxias (ADCAs) is an autosomal dominant neurodegenerative disorder characterized by a wide range of clinical manifestation, including cerebellar ataxia, pyramidal and extrapyramidal signs, progressive external ophthalmoplegia, dystonia with rigidity, and distal muscular atrophies (1,2). Mutations at different loci have been identified in ADCAs and some of the responsible genes have been cloned, including Spinocerebellar Ataxia Type 1 (SCA1) on chromosome 6p (3), Spinocerebellar Ataxia Type 2 (SCA2) on chromosome 12q (4,5,6), Spinocerebellar Ataxia Type 3 (SCA3)/ Machado-Joseph disease (MJD) on chromosome 14q (7), Spinocerebellar Ataxia Type 6 (SCA6) on chromosome 19p (8) and Spinocerebellar Ataxia Type 7 (SCA7) on chromosome 3p (9). All these spinocerebellar ataxias belong to a special class of inherited neurodegenerative diseases caused by CAG trinucleotide repeat expansion in the coding region of the respective genes (10), including Huntington's disease (11,12), dentatro-rubral-pallidolusian atrophy/Haw-River-Smith's disease (DRPLA) (13,14) and spinobulbar muscular atrophy (15).

SCA3/MJD is associated with an unstable expansion of CAG trinucleotide repeat contained in MJD1 gene (7). In normal individuals the number of repeats ranges between 12 and 44, whereas in MJD/SCA3 patients the number of repeats of the affected allele varies between 53 and 86 (16-17). Clinical examination of the variability in MJD patients has led to its classification into four subtypes (18). The type I patients tend to have the longest repeats, the earliest onset (15-30 years), and

the most rapid progression with marked pyramidal and extrapyramidal signs in addition to the common features of cerebellar ataxia and ophthalmoplegia. The age at onset of the most common Type II patients are usually between 20 and 45 years; the symptoms are limited to cerebellar and pyramidal signs. The type III patients show later onset (40-60 years) and cerebellar signs, distal amyotrophic signs, marked peripheral signs and peripheral neuropathy. The rare Type IV patients are characterized by the latest onset (>50 years) with Parkinsonism and polyneuropathy. However, typical onset of symptoms usually occurs between the ages 30 and 40 years, and symptoms are slowly progressive. Anticipation, which means increasing disease severity in successive generations, is observed in these neurodegenerative disorders (10).

The long CAG repeat leads to the expression of a protein containing multiple glutamines. The pathology is thought to arise as a consequence of a gain of function by MJD1 protein or ataxin-3 (19). The polyglutamine repeat lies close to the C-terminus of ataxin-3. Ataxin-3, estimated at 42 kDa, is the smallest of the polyglutamine disease proteins. Polyglutamine diseases are dominantly inherited, typically late-onset, fatal neurodegenerative disorders. The protein is widely expressed in neurons (20) and outside the CNS, but the mutation ultimately leads to selective neuronal loss in restricted brain regions. The nature of the toxic insult of a poly(Q) mutation and its biological consequences in each disease are unclear. However, it was shown that ataxin-3 accumulates in ubiquitinated intranuclear inclusions selectively in neurons of affected brain regions (21). Neuronal intranuclear inclusions have become the neuropathological sign of the CAG repeat diseases, but their cytotoxicity still remains controversy (22).

Even though the physiological role of either normal or mutant ataxin-3 is still under investigation, the identification of the CAG repeat mutation has enabled the prenatal diagnosis of this disorder. In this paper we described our first experience with couples requesting counseling, carrier testing and prenatal diagnosis of Machado-Joseph disease in Taiwan. We also demonstrated that both normal and expanded ataxin-3 were expressed normally even in fetal tissues.

2-2 MATERIALS AND METHODS

Subject:

A 30-year-old female, whose husband has a family history of MJD, was diagnosed in the early stage of a pregnancy. This couple received genetic counseling at our medical center. Amniocentesis was carried out at 13 weeks of gestation. Before amniocentesis, motivation and psychological tolerance were evaluated at Chungau Christian Hospital, Taiwan.

DNA isolation:

Genomic DNA was isolated from peripheral lymphocytes and amniotic fluid after primary culture for 2-3 passages by standard phenol-chloroform methods (23).

DNA analysis with non-radioactive PCR:

The CAG containing fragment of the MJD gene was amplified by PCR using primers MJD52 (7) and MJD25a (a slight modification of MJD25 with sequence ATCCATGTGCAAAGGCCAGCC) (7). PCR was performed in a final volume of 20 μ l, containing 100-200 ng of genomic DNA; 10 mM Tris-HCl (pH8.8); 1.5 mM MgCl₂; 50 mM KCl; 0.1% Triton X-100; 10% dimethylsulfoxide; 200 μ M dNTPs; 80 ng of each primer; and 3 units of Taq DNA polymerase. The DNA was denature at 95 °C for 5 min; then 30 cycles at 94 °C for 1 min, 61 °C for 1 min, and 72 °C for 1 min were performed, followed by a final extension at 72 °C for 10 min. To determine the size range of CAG repeat expansion, the PCR products were analyzed on 4% agarose gels in parallel with the 100 bp marker and visualized by ethidium bromide (EB). Allele size was determined by comparison with the 100 bp marker, assuming

that the variation in the size of the product occurs within the repetitive CAG stretch.

Identification of the CAG trinucleotide repeat expansion:

For determination of CAG trinucleotide repeat at the MJD/SCA3 locus, we ran the PCR product on polyacrylamide gel electrophoresis containing fragment of the MJD gene was amplified by PCR using primers MJD52 and MJD25a (a slight modification of MJD25 with sequence ATCCATGTGCAAAGGCCAGCC) (7). PCR was performed in a final volume of 20 μ l, containing 50 ng of genomic DNA; 10 mM Tris-HCl (pH8.8); 1.5 mM MgCl₂; 50 mM KCl; 0.1% Triton X-100; 10% dimethylsulfoxide; 250 μ M each dCTP, dGTP, and dTTP; 25 μ M dATP; 1.5 μ Ci³⁵S-alpha-dATP; 125 ng each primer; and 3 units of Taq DNA polymerase. The DNA was denatured at 95 °C for 8 min; then 30 cycles at 94 °C for 1min, 61 °C for 1 min, and 72 °C for 1 min were performed, followed by a final extension at 72 °C for 10 min. To determine the exact number of CAG repeats, the PCR products were analyzed on denaturing 6% polyacrylamide gels in parallel with a pGEM sequencing ladder (-40 primer) and were visualized by autoradiography. Allele sizes were determined by comparison with the sequence ladder and were converted to CAG unit number, assuming that the variation in size of the PCR product occurs within the repetitive CAG stretch.

Fetal fibroblasts culture conditions and treatments:

Fetal fibroblasts were grown in Modified Eagle's Medium (MEM; Gibco BRL) supplemented with 10% fetal bovin serum (FBS; Gibco BRL), 2mM L-Glutamine, 1% PS (100 000U/L Penicillin G sodium, 100mg/L Streptomycin sulfate), 1% non-essential amino acid. The medium was changed every 2 days and cells

sub-cultivated every week at a ratio of 1:2. Cells were maintained at 37 °C in a humidified atmosphere with 5% CO₂.

Preparation of cell lysates for analysis by SDS-PAGE:

The cells were harvested with trypsin-EDTA after reaching 80 % confluence as judged by microscopic examination. Cells were washed twice with phosphate buffered saline (PBS) pH 7.2, then resuspended in 500 µl of lysis buffer (5% glycerol; 1 mM sodium EDTA; 1 mM sodium EGTA; 1 mM dithiothreitol; 40 µg/ml leupeptin; 40 µg/ml aprotinin; 20 µg/ml pepstatin; 1 mM PMSF; 0.5 % Triton X-100, 1X PBS) and incubation on ice for 15 min. The cell lysate was centrifuged at 16,000 rpm for 20 min at 4 °C. Supernatant was collected, and Bio-Rad protein assay reagent was used to determine the protein concentrations.

Gel electrophoresis and immunoblot analysis:

In brief, cell lysates containing 20 µg of protein were loaded onto 10% sodium dodecyl sulfate (SDS)-polyacrylamide gels. Resolved proteins were electrophoretically transferred onto 0.2 µm nitrocellulose membranes. After blocking the membrane with 5 % nonfat milk in NaCl/Pi/0.1 % Tween 20 for 1h at RT, the antibody-binding reactions were performed in the same buffer supplemented with 1 % nonfat milk at 4 °C overnight for monoclonal anti-ataxin-3 (1:2000) (24) and at room temperature for 1h for secondary antibodies coupled to horseradish peroxidase (HRP)-conjugated goat anti-mouse IgG. Results were visualized by chemiluminescence.

2-3 RESULTS

The couple has a family history of MJD and requested molecular genetic testing after prenatal counseling at our medical center under the ethic and evaluations of psychological tolerance. The husband, with a family history of MJD, was previously identified to carry a 78 CAG repeat expansion in the MJD gene (25). However, he has not developed clinical symptoms yet. The paternal grandmother, diagnosed as a MJD patient with a 78 CAG repeats in MJD gene, is still alive. She clinically presented progressive limb and truncal ataxia, ophthalmoplegia, distal muscle atrophy, and choreoathetosis. Prominent atrophy over cerebellar hemisphere and vermis were disclosed by Brain MRI study. Axono-neuropathy was found in nerve conduction study.

Non-radioactive detection on agarose gel was applied to the MJD gene analysis. This method is faster, simpler and more cost-effective than the radioactive polymerase chain reaction analysis. The PCR products resolve clear signals on 4% agarose gels (Fig. 1). On agarose gels, two DNA fragments with lower molecular weight below 300 bp were observed in the mother of fetus, indicated as a normal subject (lane 3), while the mutant alleles were found (lanes 1, 2 and 4) from the DNA samples of paternal grandmother, father, and fetus with the mosaic DNA fragments and range around 400 bp.

Meanwhile, the fetal DNA was studied with radioactive genomic PCR for the exact number of CAG repeats. The results of radioactive genomic PCR analysis of the mother and the fetus are shown in Fig. 2. The fetal sample showed two signals of 74

and 16 CAG repeats (lane 1), demonstrating one expanded fragment and one normal fragment, compared to the mother with normal alleles of 16 and 29 CAG repeats (lane 2). It is worthy noting that the CAG repeat numbers of the father were previously identified to be 78 and 15 through radioactive PCR (25), as indicated in the bottom of figure 1. After genetic counseling regarding the results of prenatal diagnosis, the couple requested termination of pregnancy. The couple received counseling, psychological and social support. Subsequently, fetal fibroblasts were obtained for further analysis by Western blot. The expression of both normal and mutant ataxin-3 protein was demonstrated by the use of monoclonal antibody against ataxin-3 (see Fig. 3). The results showed that the expanded ataxin-3, with a molecular weight about 62 kDa, migrated at a higher position than the normal ataxin-3, with a molecular weight about 47.5 kDa.

2-4 DISCUSSION

We have successfully identified an affected MJD gene from amniocentesis sampling at 13 week's gestation. Our prenatal process was performed with similar protocol reported in other countries (26). The prenatal protocol included two counseling sessions and psycho-social evaluation of the couple and obstetrical assessment: in particular, motivations for an eventual termination and decision-making processes were evaluated. After the genetic testing, in the case of pregnancy termination, the couple received counseling, psychological and social support. In this study, we applied non-radioactive PCR and radioactive PCR analysis for prenatal diagnosis of a fetus at risk of MJD. The fetal DNA showed two PCR products with 74 and 16 CAG repeats, while the father is a pre-symptomatic individual with 78 and 15 CAG repeats on MJD alleles. Our data indicated that the size of expanded MJD gene could decrease in repeat number of fetus during transmission to further generations. This contrasts with the unidirectional expansion of the CAG repeat of the MJD gene reported by Maruyama et al. (27), but is similar to our previous results (25). In addition, application of non-radioactive genomic PCR for detection the CAG repeat range of the MJD gene has made the molecular screening of MJD mutation easier in our laboratory. However, radioactive PCR analysis was required to deduce the exact number of CAG repeats.

Our results from Western blot analysis showed that the normal and mutant ataxin-3 migrated slower than what predicted from the molecular weight, indicating possible post-translational modification(s) of ataxin-3. However, further experiments are required to verify this point. In addition, it has been demonstrated that the

expanded polyglutamine in the Machado-Joseph disease protein induces cell death in vitro and in vivo (28). Animal models have shown that truncated expanded MJD fragments can induce the formation of intranuclear inclusions, thereby causing damage at the cellular level, whereas the normal ataxin-3 protein does not (29). All these observations suggested that it is importance to understand the expression and cellular functions of ataxin-3. It was previously reported that the normal and mutant ataxin-3 are constitutively expressed in all human tissues (19). Our results further demonstrated the first time that the expression of both normal and expanded ataxin-3 was present in the fetus. However, the cellular functions of ataxin-3 and the reasons of the disease' late onset is still unclear.

In summary, we report here the first case of prenatal diagnosis of MJD in Taiwan. The diagnosis was made using a simple non-radioactive PCR for rapid detection of the presence of an expanded MJD allele. However, the accurate number of CAG expansion in MJD gene should be resolved by the use of radioactive PCR, which is a standard assay for diagnosis of SCA3. In the case of homoallelic individuals, Southern-blot method may be used to completely exclude cases of nonamplification of expanded alleles in the homoallelic individuals (30). It is noted that a reduction in CAG triplet repeats of MJD gene was found in this case of paternal-transmission. In addition, the expression of both normal and mutant ataxin-3 was detected early in the 13 weeks' fetus. In about 40% of ADCA families the genetic background of the diseases can be identified. In these families genetic testing also enables prenatal testing. However, because the cause of ADCA still remains unidentified in most families, there is a need for training genetic counselors to understand the phenotype and genotype differences in ADCA. This will certainly benefit the patients and

families with autosomal dominant cerebellar ataxias (ADCAs).

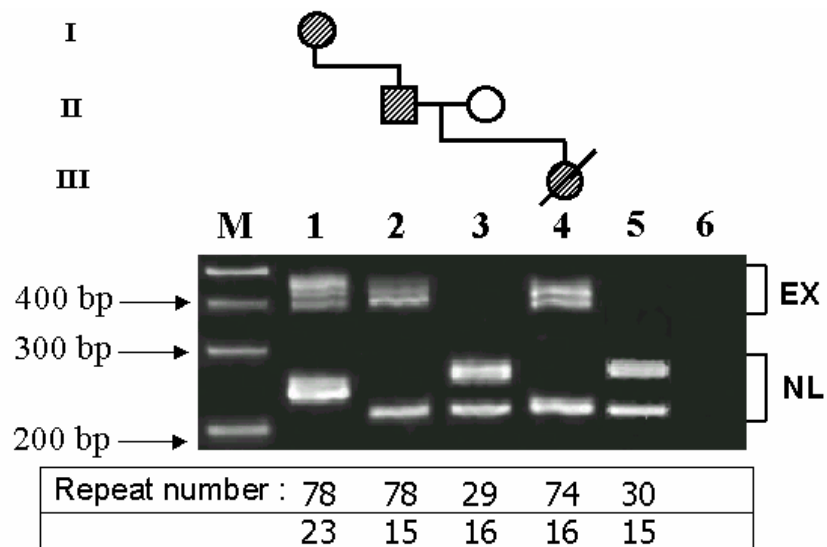


Figure1: Detection of the CAG expansion in the MJD gene on 4% agarose gel. PCR analysis of DNAs. Two DNA fragments with lower molecular weight below 300 bp were observed in the mother of fetus (lane 3) and a non-related human wild type control (lane 5), while the expanded mutant alleles were found from the samples of the paternal grandmother, father, and fetus (lanes 1, 2 and 4) with moderated mosaic DNA fragments and range around 400 bp. Lane 6, no template control; EX, expanded allele; NL, normal allele.

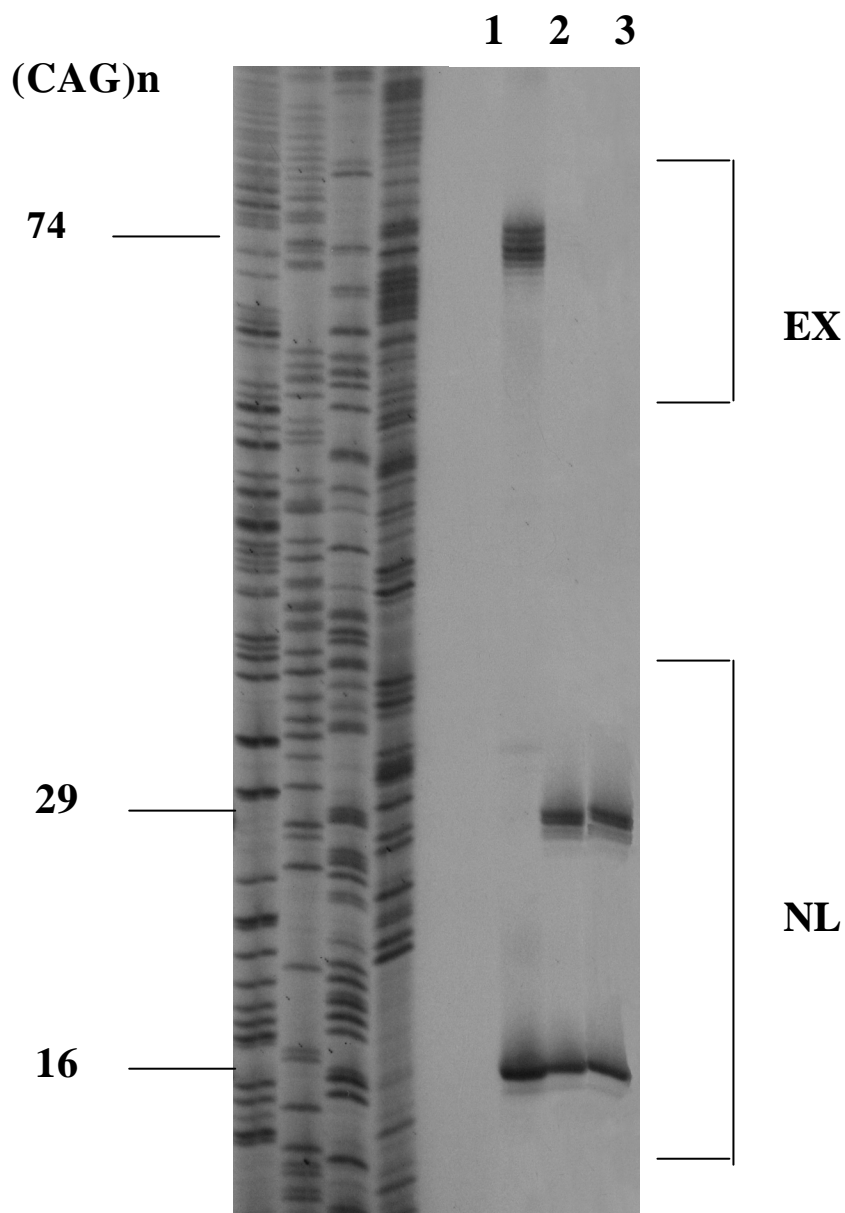


Figure 2: PCR analysis of MJD gene. PCR-amplified CAG repeats in amniocentesis sample from the fetus (lane 1), in blood DNA sample from the mother (lane 2), and a non-related human wild type control (lane 3). The four tracks on the left contain pGEM sequence, which were used to determine the size of alleles. The corresponding sizes of the alleles are indicated on the left. EX, expanded allele; NL, normal allele.

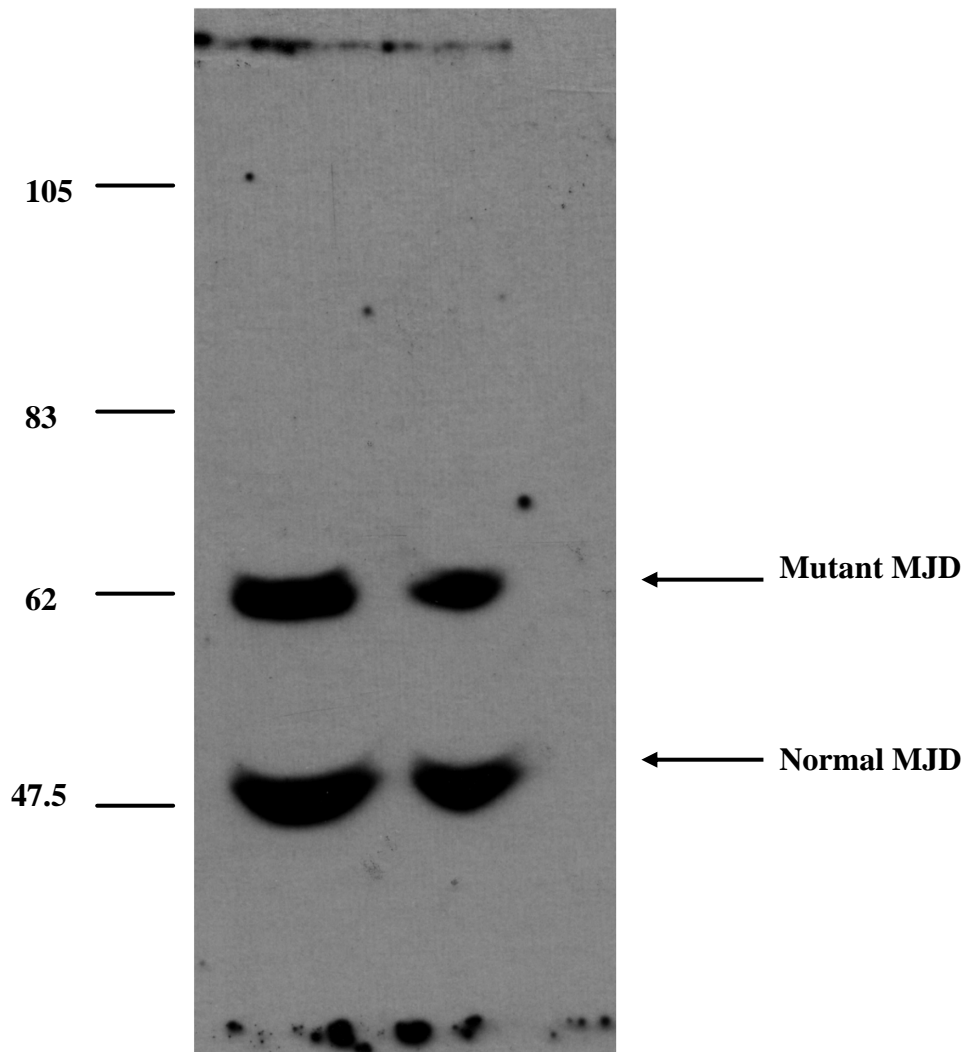


Figure 3: Detection of mutant MJD protein from fetal fibroblasts. Fetal fibroblasts were cultured and the cultured cell lysate was subjected to Western blot analysis with anti-MJD monoclonal antibody.

2-5 REFERENCES

1. Coutinho P, Calheiros JM, Andrade C. On a new degenerative disorder of the central nervous system, inherited in an autosomal dominant mode and affecting people of Azorean extraction. *O Medico* 1997; 82: 446-448.
2. Rosenberg RN. Autosomal dominant cerebellar phenotypes: the genotype has settled the issue. *Neurology* 1995; 45: 1-5.
3. Orr HT, Chung M, Banfi S, et al. Expansion of an unstable trinucleotide CAG repeat in spinocerebellar ataxia type 1. *Nat Genet* 1993; 4: 221-226.
4. Sanpei K, Takano H, Igarashi S, et al. Identification of the spinocerebellar ataxia type 2 gene using a direct identification of repeat expansion and cloning technique, DIRECT. *Nat Genet* 1996; 14: 277-284.
5. Imbert G, Saudou F, Yvert G et al. Cloning of the gene for spinocerebellar ataxia 2 reveals a locus with high sensitivity to expanded CAG/glutamine repeats. *Nat Genet* 1996; 14: 284-290.
6. Pulst SM, Nechiporuk A, Nechiporuk T, et al. Moderate expansion of a normally biallelic trinucleotide repeat in spinocerebellar ataxia type 2. *Nat Genet* 1996; 14: 269-276.
7. Kawaguchi Y, Okamoto T, Taniwaki M, et al. CAG expansions in a novel gene from Machado-Joseph disease at chromosome 14q32.1. *Nat Genet* 1994; 8: 221-227.

8. Zhuchenko O, Bailey J, Bonnen P, et al. Autosomal dominant cerebellar ataxia (SCA6) associated with small polyglutamine expansions in the 1A-voltage-dependent calcium channel. *Nat Genet* 1997; 15: 62–69.
9. David G, Abbas N, Stevanin G, et al. Cloning of the SCA7 gene reveals a highly unstable CAG repeat expansion. *Nat Genet* 1997; 17: 65–70.
10. Sutherland GR, Richards RL. Simple tandem repeats and human genetic disease. *Proc Natl Acad Sci USA* 1995; 92: 3636-3641.
11. Andrew SE, Goldberg YP, Kremer B, et al. The relationship between trinucleotide (CAG) repeat length and clinical features of Huntington's disease. *Nat Genet* 1993; 4: 398-403.
12. Huntington's Disease Collaborative Research Group. A novel gene containing a trinucleotide repeat that is expanded and unstable on Huntington's disease chromosome. *Cell* 1993; 72: 971-983.
13. Koide R, Ikeuchi T, Onodera O, et al. Unstable expansion of CAG repeat in hereditary dentatorubral-pallidolusian atrophy (DRPLA). *Nat Genet* 1994; 6: 9-13.
14. Nagafuchi S, Yanagisawa H, Sato K, et al. Dentatorubral and pallidolusian atrophy expansion of an unstable CAG trinucleotide on chromosome 12p. *Nat Genet* 1994; 6: 14-18.
15. La Spada AR, Wilson EM, Lubahn DB, Harding AE, Fischbeck KH. Androgen receptor gene mutations in X-linked spinal and bulbar muscular atrophy. *Nature*

1991; 352:77-79.

16. Sinden RR. Biological implication of the DNA structure associated with disease-causing triplet repeats. *Am J Hum Gene* 1999; 64: 346-353.
17. Van Alfen N, Sinke RJ, Zwarts MJ, et al. Intermediate CAG repeat lengths (53, 54) for MJD/SCA3 are associated with an abnormal phenotype. *Ann Neurol*. 2001; 49: 805-807.
18. Lopes-Cendes I, silveira I, Maciel P, et al. Limits of clinical assessment in the accurate diagnosis of Machado-Joseph disease. *Arch Neurol* 1996; 53: 1168-1174.
19. Takiyama Y, Oyanagi S, Kawashima S, et al. A clinical and pathologic study of a large Japanese family with Machado-Joseph disease tightly linked to the DNA markers on chromosome 14q. *Neurology* 1994; 44: 1302-1308.
20. Gutekunst CA, Li SH, Yi H, et al. Nuclear and neuropil aggregates in Huntington's disease: relationship to neuropathology. *J Neurosci* 1999; 19: 2522-2534.
21. Paulson HL, Perez MK, Trottier Y, et al. Intranuclear inclusions of expanded polyglutamine protein in spinocerebellar ataxia type 3. *Neuron* 1997; 19: 333-344.
22. Yamada M, Tsuji S, Takahashi H. Pathology of CAG repeat diseases. *Neuropathology* 2000; 20: 319-325.

23. Ko TM, Tseng LH, Hsieh FJ, Hsu PM, Lee TY. Carrier detection and prenatal diagnosis of alpha-thalassemia of Southeast Asian deletion by polymerase chain reaction. *Hum Genet* 1992; 88: 245-248.
24. Wang G, Ide K, Nukina N, et al. Machado-Joseph disease gene product identified in lymphocytes and brain. *Biochem Biophys Res Comm* 1997; 233: 476-479.
25. Hsieh M, Tsai HF, Lu TM, Yang CY, Wu HM, and Li SY. Studies of the CAG repeat in the Machado-Joseph disease gene in Taiwan. *Hum Genet* 1997; 100: 155-162.
26. Sequeiros J, Maciel P, Taborda F, et al. Prenatal diagnosis of Machado-Joseph disease by direct mutation analysis. *Prenat Diagn* 1998; 18: 611-617.
27. Maruyama H, Nakamura S, Matsuyama Z, et al. Molecular features of the CAG repeats and clinical manifestation of Machado-Joseph disease. *Hum Mol Genet* 1995; 4: 807-812.
28. Ikeda H, Yamaguchi M, Sugai S, Aze Y, Narumiya S, and Kakizuka A. Expanded polyglutamine in the Machado-Joseph disease protein induces cell death in vitro and in vivo. *Nat Genet* 1996; 19: 196-201.
29. Chai Y, Koppenhafer SL, and Paulson HL. Analysis of the role of heat shock protein molecular chaperones in polyglutamin disease. *J Neurosci* 1999; 19: 10338-10347.
30. Maciel P, Costa MC, Ferro A, et al. Improvement in the molecular diagnosis of Machado-Joseph disease. *Arch Neurol* 2001; 58: 1821-1827.

Chapter 3: Full-length expanded ataxin-3 enhances mitochondrial-mediated cell death and decreases Bcl-2 expression in human neuroblastoma cells

ABSTRACT

Machado-Joseph disease (MJD) is an autosomal dominant spinocerebellar degeneration characterized by a wide range of clinical manifestations. An unstable CAG trinucleotide repeat expansion in MJD gene on long arm of chromosome 14 has been identified as the pathologic mutation of MJD and apoptosis was previously shown to be responsible for the neuronal cell death of the disease. In this study, we used human neuronal SK-N-SH cells stably transfected with HA-tagged full-length MJD with 78 polyglutamine repeats to examine the effects of polyglutamine expansion on neuronal cell survival in the early stage of disease. Various pro-apoptotic agents were used to assess the tolerance of the mutant cells and to compare the differences between cells with and without mutant ataxin-3. Concentration- and time-dependent experiments showed that the increase in staurosporine-induced cell death was more pronounced and accelerated in cells containing expanded ataxin-3 via MTS assays. Interestingly, under basal conditions, Western blot and immunocytochemical analysis showed a significant decrease of Bcl-2 protein expression and an increase of cytochrome c in cells containing expanded ataxin-3 when compared with those of the parental cells. The same reduction of Bcl-2 was further confirmed in fibroblast cells with mutant ataxin-3. In addition, exogenous expression of Bcl-2 desensitized SK-N-SH-MJD78 cells to poly-Q toxicity. These results indicated that mitochondrial-mediated cell death plays a

role in the pathogenesis of MJD. In our cellular model, full-length expanded ataxin-3 that leads to neurodegenerative disorders significantly impaired the expression of Bcl-2 protein, which may be, at least in part, responsible for the weak tolerance to polyglutamine toxicity at the early stage of disease and ultimately resulted in an increase of stress-induced cell death upon apoptotic stress.

3-1 INTRODUCTION

Machado-Joseph disease (MJD) belongs to a special class of inherited neurodegenerative disease caused by CAG trinucleotide repeat expansion in the coding region of the respective genes, in all cases, the CAG repeats are transcribed and translated into polyglutamine tracts (1). Polyglutamine diseases are dominantly inherited, typically late-onset, fatal neurodegenerative disorders. All MJD affected patients exhibit expanded CAGs with 55 to 84 repeats whereas 13 to 51 repeats for normal individuals (2). An inverse correlation between the expanded repeat length and the age-at-onset of the trinucleotide disease has been reported in MJD (3). It has been demonstrated that both normal and mutant ataxin-3 proteins were expressed throughout the body and in all regions of the brain (4). Although this protein is widely expressed in neurons (5) and outside the central nervous system (CNS), its mutation ultimately leads to selective neuronal loss in restricted brain regions. Recently, it was reported that ataxin-3 is a histone-binding protein with two independent transcriptional corepressor activities (6), however, the specific targets of ataxin-3 in the pathogenesis of MJD remains to be addressed. It was shown that the ataxin-3 accumulates in ubiquitinated intranuclear inclusions specifically in neurons of affected brain regions (7). Although neuronal death is an essential feature in Machado-Joseph disease and there was evidence to show that expanded ataxin-3 could sensitize cells to apoptosis, most studies have come from the overexpression of N-terminal truncated expanded ataxin-3 in non-human neuronal cell lines (8-10). The pathogenesis and molecular basis of how the full-length expanded ataxin-3 leads to neuronal cell death in Machado-Joseph disease still remains unclear.

Staurosporine (STS), a potent and non-specific inhibitor of protein kinase C (11), has been shown to be capable of inducing mitochondrial-mediated apoptotic cell death, which is a process of cell death mediated by caspases (12,13) and 14 family members of caspases have been identified so far (14). At least in some cell types, signals originating from death receptors require the mitochondria, and thus depend on the Bcl-2 family of proteins (15). Overexpression of Bcl-2 proteins has been shown to be able to inhibit apoptosis by preventing the activation of caspase-9, which is crucial for cell death and the major apoptotic pathway activated by cytotoxic stimuli (16). Expression of pro- or antiapoptotic proteins of the Bcl-2 family may modify the sensitivity to induce apoptosis and control the survival of neurons (17). Some components, such as Bcl-2 and Bcl-xL, may suppress apoptosis, while others, such as Bax and Bid, may have an enhancing effect. The overexpression of antiapoptotic Bcl-2 in neuronal cells was shown to prevent programmed cell death both *in vitro* and *in vivo* (18,19) and the overexpression or inactivation of one component of the Bcl-2 protein family could drastically modify the sensitivity to apoptosis and greatly alter other parameters involved in cell physiology (20,21).

Previously, experiments performed in primary striatal neurons showed that the polyglutamine cytotoxicity can be inhibited by the anti-apoptotic protein Bcl-xL and caspase inhibitors (22) and involvement of caspases has also been indicated in HD transgenic mice model (23) and in HD lymphoblasts (24). In the present study, human neuroblastoma SK-N-SH cell line (containing endogenous normal ataxin-3 with 26 glutamine residues), expressing the oncoproteins of the Bcl-2 family (11), was used as a parent cell line. SK-N-SH-MJD78 cells, SK-N-SH being stably transfected with HA-tagged full-length MJD with 78 polyglutamine repeats (25), were used to examine the effects of polyglutamine expansion on the survival of neuronal cells, as

well as Bcl-2 protein expression, under various apoptotic stresses to explore the mechanism for MJD pathogenesis at the early stage of disease. Our results indicated that cells containing expanded full-length ataxin-3 were more susceptible to the staurosporine-induced apoptotic insult, compared to cells without expanded ataxin-3. In addition, here we demonstrated that the expression of full-length mutant ataxin-3 does not dramatically elevate cell death under basal conditions, but does significantly impair the protein expression of Bcl-2 under normal growth conditions. The decrease of Bcl-2 protein may modify drastically the sensitivity to apoptosis and alter greatly other parameters that eventually disrupt cell physiology in MJD patients. These may explain, at least in part, the increased stress-induced cell death upon aging.

3-2 MATERIALS AND METHODS

Cell lines and Reagents:

SK-N-SH cells were provided by Dr. Shin-Lan Hsu (Taichung Veterans General Hospital, Taiwan); SK-N-SH-MJD78 cells were obtained from previous study (25). Fibroblast cells from a MJD fetus and a normal control were obtained from previous study (26). The cDNA clone encoding full-length human Bcl-2 was a kind gift from Dr. Shie-Liang Hsieh [27]. All materials for cell culture were obtained from Gibco Life Technologies (Gaithersburg, MD). Reagents for western blot were obtained from Pierce (Rockford, USA). Mouse monoclonal antibodies specific for Bcl-2, Bad, Bcl-xL (BD Transduction Laboratories, Lexington, KY), Bax (Santa Cruz Biotechnology, Santa Cruz, CA), Cytochrome c (Labvision, CA). Monoclonal anti-actin was from Sigma (St Louis, MO). All other supplies were obtained from Sigma Chemical (St Louis, MO).

Cell culture conditions :

The human fetal fibroblast cells and neuroblastoma cells were grown in DMEM medium supplemented with 10% fetal bovine serum (FBS), 2 mM L-Glutamine, 1% PS, 1% non-essential amino acid and maintained at 37 °C in a humidified atmosphere with 5% CO₂. The cells were sub-cultivated every three days at a ratio of 1:2.

Cell toxicity studies and cell survival analysis:

SK-N-SH and SK-N-SH-MJD78 cells were maintained in DMEM medium containing 10% fetal bovine serum and then prepared at a concentration of 1x10⁵ cells/ml, 100µl of which was added to each well of 96-well plates. One day after seeding, cultured medium was replaced with a medium containing STS (0, 1 or 2 µM)

and cells were incubated in this medium for various periods, including 12, 24, 36, 48, and 60 h, at 37 °C and then harvested for a cell viability analysis by a modified 3-(4,5-dimethylthiazol-2-yl)-2,5-diphenyltetrazolium bromide (MTS) assay (Cell titer 96, Promega) as described previously (28). At least 6 cultures for each time point were assayed. After an incubation of 4 h, optical densities were measured at 490 nm and results were expressed as percentage of controls.

Characterization of apoptosis:

Control or drug-treated cells were harvested by trypsin incubation, washed in phosphate buffer saline (PBS), fixed with 4% paraformaldehyde in PBS buffer for 30 min at room temperature (RT), exposed to 10 µg/ml 4',6-diamidino-2-phenylindole (DAPI) in PBS for 5 min at 37 °C, washed three times with PBS mounted with Cytoseal™60 Mounting Medium, and finally examined under UV illumination on a Nikon fluorescence microscope. Condensed or fragmented DNA appeared as highly fluorescent in apoptotic cells.

Immunoblot analysis:

The cells were harvested with trypsin-EDTA after reaching 80 % confluence as judged by microscopic examination. Cells were washed twice with phosphate buffered saline (PBS) pH 7.2, then resuspended in 500µl of lysis buffer (5% glycerol; 1 mM sodium EDTA; 1 mM sodium EGTA; 1 mM dithiothreitol; 40 µg/ml leupeptin; 40 µg/ml aprotinin; 20 µg/ml pepstain; 1 mM PMSF; 0.5 % Triton X-100, 1X PBS) and incubation on ice for 15 min. The cell lysate was centrifuged at 16,000 rpm for 20 min at 4 °C. Supernatant was collected, and Bio-Rad protein assay reagent was used to determine the protein concentration. Cell lysates containing a total protein of 20-30 µg were loaded onto 12% SDS-polyacrylamide gels. Resolved proteins were then

electrophoretically transferred onto nitrocellulose membranes. After blocking the membrane with 5% nonfat milk in NaCl/Pi/0.1% Tween 20 for 1h at room temperature, all antibody-binding reactions were performed in the same buffer supplement with 1% nonfat milk at 4 °C overnight for primary antibodies and at room temperature for 1h for secondary antibodies conjugated with a horseradish peroxidase. The signal was detected by the enhanced chemiluminescence Western blot system (Pierce). A monoclonal antibody against β -actin was included in the experiments for an internal control.

Immunocytochemistry:

Cells, collected using cytospin, were fixed with 4% paraformaldehyde in 0.1 M phosphate-buffered saline (pH 7.4) for 20 min. They were treated with 0.3% H₂O₂ in 100% ethanol for 10 min to eliminate endogenous peroxidase and incubated with 10% normal goat serum (ABC kit, Zymed, South San Francisco, CA) for 1 h at 37 °C. Cells were incubated with Bcl-2 antibodies (1:100) in 10% normal goat serum overnight at 4 °C. After primary incubation, cells were treated with biotinylated secondary antibodies (DAKO) for 1 h at 37 °C, followed by incubation with a streptavidin peroxidase conjugate (DAKO) for 1 h at 37 °C. Immunolabels were visualized with 3,3'-diaminobenzidine staining kit (Zymed, South San Francisco, CA) and counter-stained with Meyer's Hematoxylin.

Assay for cytochrome c in the cytosol:

Levels of cytochrome c in the cytosol were examined according to the manufacturer's instructions (CNM compartment protein extraction kit; BioChain, CA).

Isolation of total RNA and semi-quantitative reverse-transcriptase PCR (RT-PCR):

Total RNA was extracted from cells using Trizol reagent (Life Technologies, USA). For each sample, 3 µg of RNA was reverse-transcribed into cDNA in a final volume of 20 µl with 50 pmol oligo d(T) and 50 units MMLv reverse transcriptase (Perkin Elmer, USA) for 15 min at 42 °C. The mRNA for bcl-2 and G3PDH were measured by semi-quantitative RT-PCR. The primers used were: bcl-2 upstream 5'-CGACGA CTTCTCCCGCCGCTACCGC-3', bcl-2 downstream 5'-CCGCATGCTGGG GCCGTACAGTTCC-3'; G3PDH upstream 5'-CCATGTTCGTCATGGGTG TGAACCA-3', downstream 5'-GCCAGTAGAGGCAGG GATGATGTTC-3'. PCR was performed in a final volume of 25 µl using 5 µl from the RT reaction for cDNA amplification. The PCR mixture contained 20 pmol each of upstream and down stream primers and 1 unit Taq polymerase (Promega, USA). Conditions for the PCR were as the followings: an initial denature for 5 min at 94 °C, followed by 30 s at 94 °C, 1 min at 72 °C, for 30 cycles. A sample without RNA was included in each experiment of RT-PCR as a negative control. Ethidium bromide-stained PCR products were separated on 3% agarose gels, visualized and quantified using a LAS-1000 plus imaging analyzer (Fujifilm, Japan). The sizes of the amplified products were 319 bp and 251 bp for Bcl-2 and G3PDH, respectively. In order to compare the amplified products semi-quantitatively, quantitation of the signals was performed using a densitometric scanner. The use of G3PDH provided good control of the bias caused by possible degradation of the mRNA. We had earlier confirmed after 30 amplification cycles that the RT-PCR reactions were in a linear range and not at a plateau (data not shown).

Transient-transfection assays:

Transient-transfection was performed in exponentially growing SK-N-SH and

SK-N-SH-MJD78 cells, plated one day before transfection in 6-well plates (2×10^5 cells/well). For double-transfection experiments (Bcl-2 overexpression and pEGFP), we used a 4:1 ratio of test DNA and 20 μ l of Lipofectamine (Invitrogen-Life Technologies) which were preincubated for 45 minutes and then added to the cells. After 3 hours, the Optimum DNA mixture was replaced with complete growth medium, and cells were analysed for with staurosporine (STS) 24 hours later. At 48 hours after transfection, cells on coverslips were fixed with 4% paraformaldehyde in $1 \times$ PBS at room temperature for 20 minutes and mounted in antifadent supplemented with 4', 6-diamidino-2-phenylindole (DAPI) (10 μ g/ml) to allow visualization of nuclear morphology. The transfection efficiency (50-80%, depending on the cell line) was compared in parallel experiments using pEGFP.

Statistical analysis:

All bands were quantified by laser densitometry and values were expressed as mean \pm SEM. Analysis of variance with subsequent Student's t test was employed to determine the significance of differences in comparisons. Values of $P < 0.05$ were considered statistically significant.

3-3 RESULTS

Expanded ataxin-3 led to a decrease in the number of viable cells upon staurosporine treatment

SK-N-SH-MJD78 is a human neuroblastoma cell line that was established previously in our laboratory for the studies of early events in the presence of expanded full-length ataxin-3 (25). To determine which apoptotic pathway may be involved in the early stage of MJD pathogenesis, we examined cell viability in response to different apoptotic stimuli in this model system. Human SK-N-SH cells, containing endogenous normal ataxin-3 with 26 glutamine residues, were used as the parental cells. SK-N-SH cells and SK-N-SH-MJD78 cells were first treated with brefeldin A and tunicamycin, which can induce effective cleavage of procaspase-12, and then assayed by MTS/PMS test. The results indicated no significant differences between cells with and without mutant ataxin-3 in response to up to 10 $\mu\text{g/ml}$ of brefeldin A or tunicamycin for up to 96 h (data not shown). Furthermore, SK-N-SH and SK-N-SH-MJD78 cells were treated with staurosporine (STS), a non-endoplasmic reticulum (ER) stress inducing apoptotic stimulus, to result in a dose-dependent reduction (Fig. 1A), as well as a time-dependent reduction (Fig. 1B), in the number of viable cells in both SK-N-SH and SK-N-SH-MJD78 cells. It was noted that cells expressing expanded ataxin-3 were more sensitive to the non-ER stimuli, as evidenced by more dramatic decrease of cell viability under the treatment of 1 μM STS (Fig. 1A). After a 12-hour treatment of STS, the number of viable SK-N-SH-MJD78 cells was decreased to approximately 40% of the untreated while parental SK-N-SH cells preserved 80% viability under the same condition. The results indicated that, non-ER stress may be involved in the early pathogenesis of MJD. To investigate whether the change in the number of viable cells was related to the

occurrence of apoptosis, cell morphological change upon the drug treatment was studied next.

Staurosporine induced more apoptotic MJD cells

A hallmark of apoptosis is nucleosomal fragmentation of DNA. To determine whether a decreased number of viable cells associated with the occurrence of apoptosis and whether STS induced apoptosis in SK-N-SH-MJD78 cells was more pronounced than that in parental cells, DNA fragmentation was studied with microscopic observations. The apoptotic sensitivity of SK-N-SH-MJD78 cells was evaluated after a 24-hour incubation with 0 and 1 μM of STS as shown in Figure 1C. The ability of cells to undergo apoptosis was estimated by fluorescence microscope after washing, fixing cells with 4% formaldehyde (w/v) and DAPI staining where the chromatin in nuclei of apoptotic cells appeared condensed, glossy, or fragmented. A quantitative assessment of the percentage of apoptotic cells was illustrated in Fig. 1D. After a STS treatment for 24 hours, the treated SK-N-SH-MJD78 cells produced large numbers of apoptotic cells exclusively with highly fragmented nuclei even under a low concentration of STS treatment (0.5 μM) whereas untreated control SK-N-SH and SK-N-SH-MJD78 cells both showed very few condensed nuclei without fragmentation. However, STS-treated SK-N-SH cells produced significant apoptotic cells only upon a higher concentration of STS treatment (1 μM) (Fig. 1D). It was worth to note that due to the low viability, the cell numbers of SK-N-SH-MJD78 were significantly lower than those of the parental cells upon the STS treatment under the microscope observation. The results demonstrated that STS induced apoptosis of SK-N-SH-MJD78 cells more rapidly than that of parental cells. STS caused a dose-dependent increase in apoptosis in SK-N-SH-MJD78 cells.

Decreased Bcl-2 expression in cells containing mutant MJD proteins

In order to investigate the origins of these changes in the sensitivity to apoptosis induced by STS, an analysis of the Bcl-2 family, known to be implicated in the control of apoptosis, was carried out. Under normal growth conditions, Western blot analysis demonstrated that the protein levels of Bcl-2 in SK-N-SH-MJD78 cells significantly decreased as compared to the parental cells (Fig. 2A). To confirm that the altered expression of Bcl-2 was specific, β -actin was included as the internal control. A quantitative assessment of the percentage of protein expression revealed that Bcl-2 in MJD cells retained only about 33 % of that of the parental cells (Fig. 2B). This observation was further confirmed by immunocytochemical staining using mouse monoclonal antibodies against Bcl-2. As shown in Fig. 2C, significant staining differences were observed in cells containing expanded ataxin-3, compared with the parental cells. Our results demonstrated that the protein level of Bcl-2 was significantly decreased in the presence of expanded ataxin-3 in the cellular system.

Expression of Bcl-2 protein family under normal conditions

To further study the molecular mechanisms of apoptosis in SK-N-SH-MJD78 cells, we compared the expression of other Bcl-2 family members in our cellular model. Bax and Bcl-2 are homologous proteins that have opposing effects on cells, with Bcl-2 serving to prolong cell survival while Bax acting as an accelerator of apoptosis (29). Conversely, proapoptotic protein levels of Bax showed unchanged in cells with and without expanded ataxin-3 as examined by Western blot analysis (Fig. 2D). Our results showed that expanded ataxin-3 did not significantly modify Bax expression while the ratio of Bcl-2 to Bax decreased in the presence of expanded ataxin-3, which indicated that mutant cells are prone to apoptotic stress. In addition, protein expression levels of Bad and Bcl-xL were also examined under the same

growth conditions. The expression of Bcl-xL and Bad did not differ significantly between cells with and without expanded ataxin-3 (Fig. 2E). These results indicated that the altered protein expression of Bcl-2 was specific in the cellular model.

Decreased Bcl-2 expression in MJD fetal fibroblast cells

In order to understand whether the altered expression of Bcl-2 is also reproducible in different cell types of various human tissues, skin fibroblast cells from one MJD fetus (26) and one normal control fetus were used for comparison. Western blot analysis further confirmed a significant reduction of Bcl-2 in MJD fibroblast cells, compared with that from normal fetal fibroblast cells (Fig. 3). Meanwhile, protein expression levels of Bad and Bcl-xL were also examined, and our results showed that the expression of Bcl-xL and Bad did not differ significantly between the MJD fetus and the normal control.

Increased cytochrome c expression in SK-N-SH-MJD78 cells

Another hallmark of apoptotic program, cytochrome *c* release, was also examined in the *in vitro* cellular system. Our results demonstrated that level of cytochrome *c* releasing from mitochondria in cells containing mutant ataxin-3 was increased (lane 2 of Fig. 4), comparing to that of the parental cells (lane 1 of Fig. 4). Therefore, Western blot analyses of the molecular factor mediating apoptosis via the mitochondrial pathway showed that Bcl-2 down-regulation and cytochrome *c* release were significantly affected by the presence of mutant ataxin-3 in SK-N-SH-MJD78 cells. Next, we determined whether this reduction in Bcl-2 was at the transcriptional level. Semiquantitative RT-PCR revealed that an 80% decrease in Bcl-2 mRNA levels was observed in cells expressing mutant ataxin-3 as compared to that of the parental cells, with G3PDH being an internal control (Fig. 5). This observation suggested that

the down-regulation of Bcl-2 protein could be due to the defects at the transcriptional level. Since polyglutamine may exert proapoptotic effects through a down-regulation of Bcl-2, whether overexpression of Bcl-2 may desensitize SK-N-SH-MJD78 cells to poly-Q toxicity was investigated. As shown in Figure 6, exogenous expression of Bcl-2 in SK-N-SH-MJD78 cells, which have been transiently transfected with Bcl-2 overexpression plasmids together with a control plasmid, pEGFP, markedly reduced the apoptotic cells upon the STS treatment. Our results indicated that Bcl-2 overexpression significantly reduced polyglutamine-induced cell death of SK-N-SH-MJD78 cells.

3-4 DISCUSSION

Although an inducible rat mesencephalic CSM14.1 clonal cell line expressing expanded human full-length ataxin-3 was previously reported (30), a human neuronal cell line expressing mutant full-length ataxin-3 would be valuable to study the effect of mutant ataxin-3. In the present study, we utilized human neural SK-N-SH-MJD78 cells that have been stably transfected with polyglutamine expansion constructs (25) to analyze the role(s) of expanded full-length ataxin-3 may play in response to various apoptotic stimuli. In contrast to transient transfection or inducible polyglutamine expression, cells in the present study do not undergo a rapid form of cell death under basal conditions. It is interesting to note that the ability of neuronal cells to withstand the existence of expanded ataxin-3 for prolonged periods without apparent adverse effects in our cellular model. With very few SK-N-SH-MJD78 cells containing nuclear aggregates (25), our model system represents an early stage of disease, which may be particularly important for studying the initiation events of polyglutamine cytotoxicity in human neuronal cells.

Although neuronal death is an essential feature in Machado-Joseph disease and there was evidence of expanded ataxin-3 sensitizing cells to apoptosis, most of the studies have come from the overexpression of N-terminal truncated expanded ataxin-3 in non-human neuronal cell lines (8-10). Which apoptotic signal that leads to full-length mutant ataxin-3 mediated cell death still remained unclear. In order to understand which apoptotic signaling pathway is responsible for the pathogenesis of MJD, SK-N-SH-MJD78 and the parental cells were treated with either non-ER stress-inducing apoptotic stimulus, staurosporine or ER stress-inducing apoptotic stimuli, such as bafeldin A and tunicamycin. Our results indicated that non-ER stress

induced more apoptotic cell death in the presence of mutant ataxin-3. This may indicate that the classical apoptotic pathway may be responsible, at least in the early stage of the disease, for the mutant ataxin-3 mediated cell death. However, upon the appearance of nuclear inclusions during the late stage of the disease, it is possible that different apoptotic-signaling pathway will be also initiated by the complexity of the disease. It was suggested earlier that the ER stress, not caused by accumulation of unfolded monomeric or oligomeric poly (Q), but is caused by large poly (Q) aggregates and inclusion themselves (31). It may be one of the apoptotic pathways induced by poly Q aggregates at the late stage of disease.

Various evidences have suggested that apoptosis plays a crucial role in cell population homeostasis that depends on the expression of various genes implicated in the control of cell life and death. It was of interest in the present study to determine if expanded ataxin-3 altered gene expression that leads to cell apoptosis observed in this cell culture system. We recently demonstrated that protein level of HSP27 was significantly decreased in cells expressing expanded ataxin-3 (25). Cells with expanded ataxin-3 were more susceptible to exogenous oxidative stress than the parental cells, indicating that these cells had weaker protection effects upon the extracellular oxidative stress (25). In addition, it was demonstrated that regulation of mitochondrial and/or cytosolic reactive oxygen intermediates (ROI) levels could be mediated, in part, by the Bcl-2 gene product (32). Expression of Bcl-2 protein prevented the induction of apoptosis by a variety of oxidative stresses, including inhibition of GSH synthesis, ionizing radiation, and heat shock (32, 33). Therefore, we examined if mutant ataxin-3 was connected to signal networks that regulate cell death, first of all, the expression levels of Bcl-2. As shown in Fig. 2, our results demonstrated that mutant MJD cells under normal conditions showed a significant

decreased Bcl-2 level when compared to the parental cells. Furthermore, a significant reduction of Bcl-2 was also observed in non-neuronal cells (fibroblast cells) expressing expanded MJD (Fig. 3). It ruled out the possibility that the reduction of Bcl-2 was the result from over-expression of a certain protein in SK-N-SH cells. Additionally, we demonstrated that increased expression of Bcl-2 could desensitize SK-N-SH-MJD78 cells to poly-Q toxicity, as evidenced by decreased apoptotic cells upon STS treatment (Fig. 6). In addition to the expression of Bcl-2, we also examined the expression of Bax, as these two homologous proteins have opposing effects on cells. However, there was no significant change in Bax expression. Since it is well known that Bcl-2 inhibits cell death induced by a variety of stimuli, mutant ataxin-3 may cause neuronal apoptosis through a down-regulation of Bcl-2, but not an up-regulation of Bax. Consistent to our observation, cells expressing mutant ataxin-3 had a significant increase of apoptotic cells compared to the untransfected control, while treated with STS (Fig. 1). In addition, our study revealed that cells expressing mutant ataxin-3 showed a significant increase in cytochrome c as compared to the control cells (Fig. 4). Taken together, these data suggested that pro-apoptotic activity related to mutant ataxin-3 utilized the classical apoptotic pathway, at least in the early stage of disease. Therefore, we hypothesized that mutant ataxin-3 induced cell apoptosis was accompanied, at least in part, by a significant decrease in Bcl-2 protein expression which led to an increase of cytochrome c released from mitochondria and finally activated the executive caspase 3 (Fig. 6). But are these the only candidates involved in the apoptotic signaling in the early stage of MJD? The growing evidence suggested not likely. For examples, heat shock proteins, acting at multiple steps in the pathway to modulate apoptosis, were shown to be involved in the pathogenesis of MJD (25, 34, 35). The small heat shock protein HSP27, similar to Bcl-2, has strong anti-apoptotic properties and functions at multiple steps of the apoptotic-signaling

pathway. It was recently shown that the altered expression of HSP27 was observed in the presence of expanded ataxin-3 (25, 36, 37). Therefore, it was possible that lack of different anti-apoptotic proteins in the early stage of the disease cells may eventually lead to cell apoptosis (Fig. 6). However, the involvement of mutant ataxin-3 in the regulation of Bcl-2 was still uncertain and the causal relationship between neuron loss and the onset of neurological dysfunction in SCA3 remains unclear, which warrants further analysis for a better understanding.

(A)

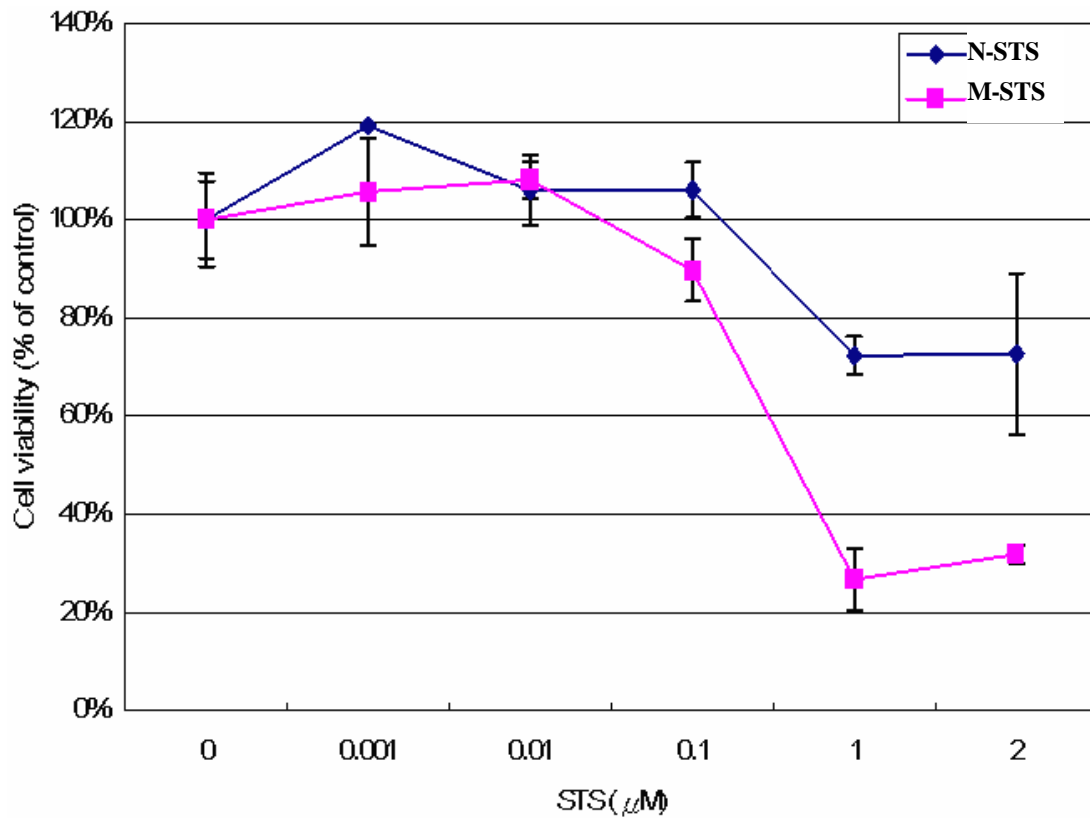


Fig. 1. (A) A concentration-dependent induction of cell death by staurosporine treatment in SK-N-SH and SK-N-SH-MJD78 cells. Cells were seeded at a density of 1×10^5 cells/ml onto 96-well plates (100 μl per well) and treated with staurosporine in the range of $1 \times 10^{-3} \sim 1 \times 10^2$ μM . After a staurosporine treatment for 24 h, cell viability was measured by MTS assays. The survival percentage was obtained by referring these values to the untreated control cells. Data were expressed as mean \pm SD from three separate experiments.

(B)

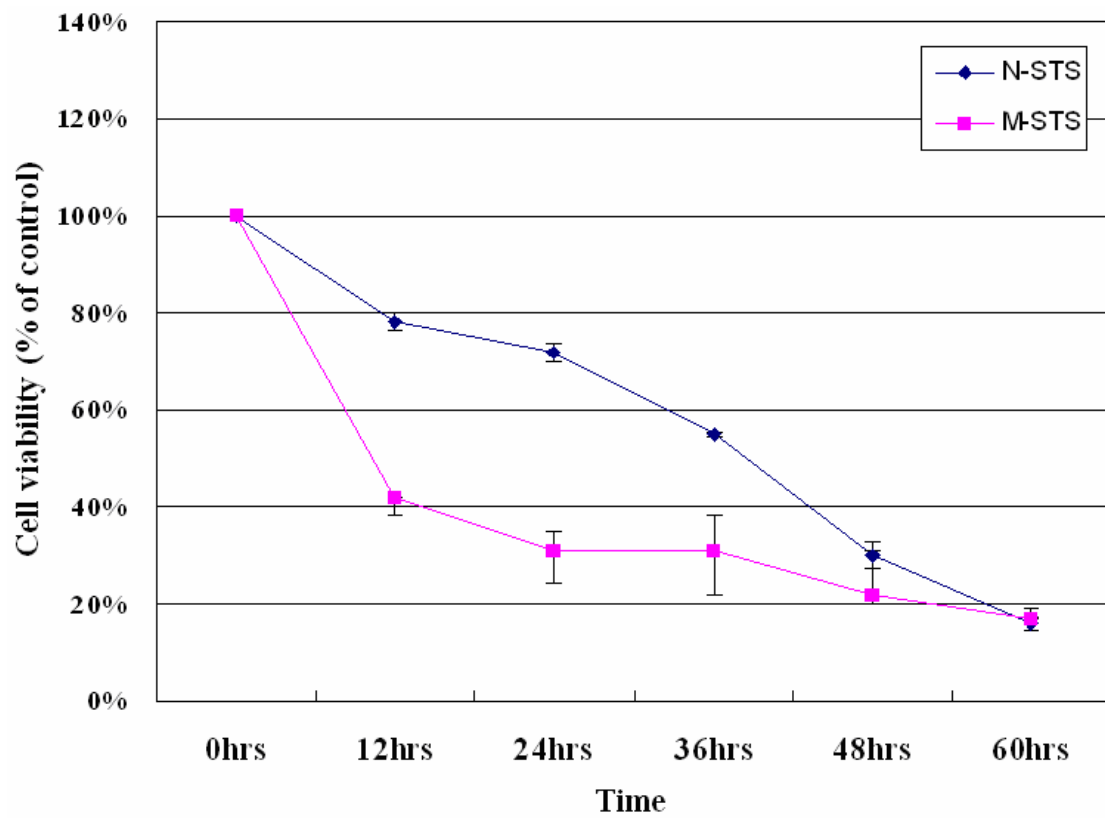


Fig. 1. (B) A time-dependent induction of cell death by staurosporine (1 μ M) treatment in SK-N-SH and SK-N-SH-MJD78 cells.

(C)

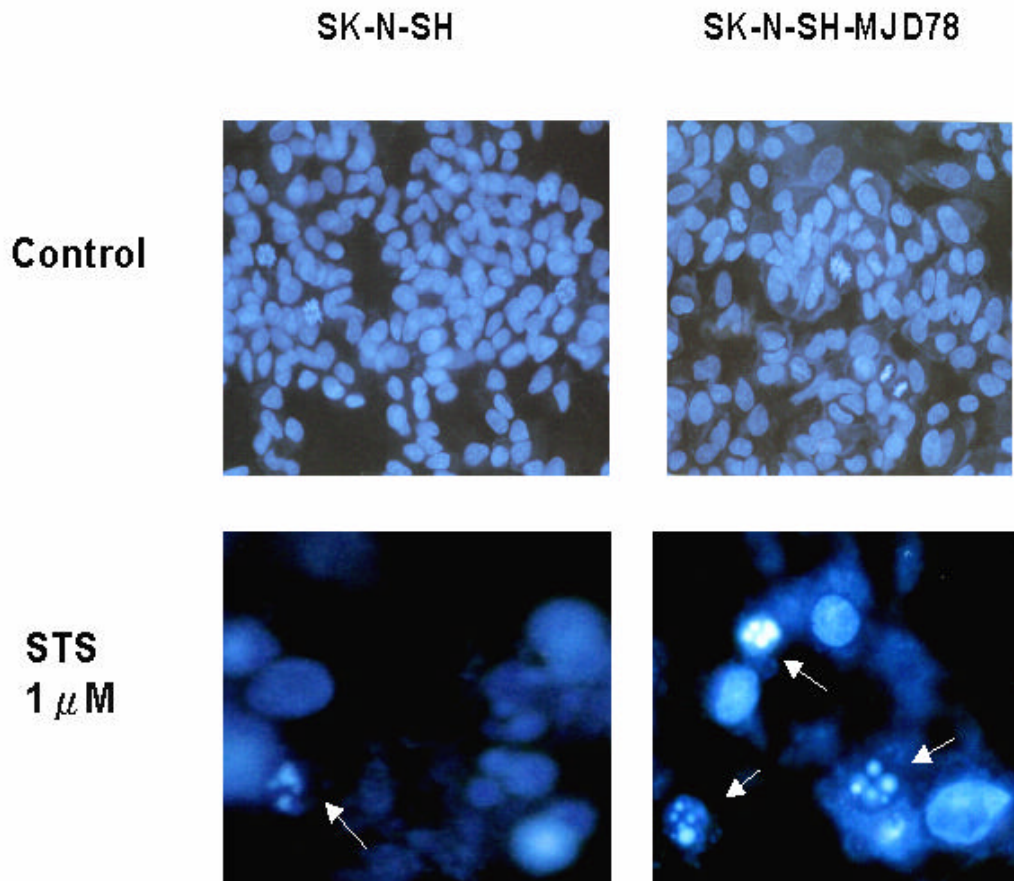


Fig. 1. (C) Microscopic observation of staurosporine-treated or untreated SK-N-SH and SK-N-SH-MJD78 cells. Staurosporine of 0 and 1 μ M, was added for a 24 h treatment and afterwards, cells were fixed with 4% formaldehyde (w/v) and then incubated with DAPI (10 μ g/ml).

(D)

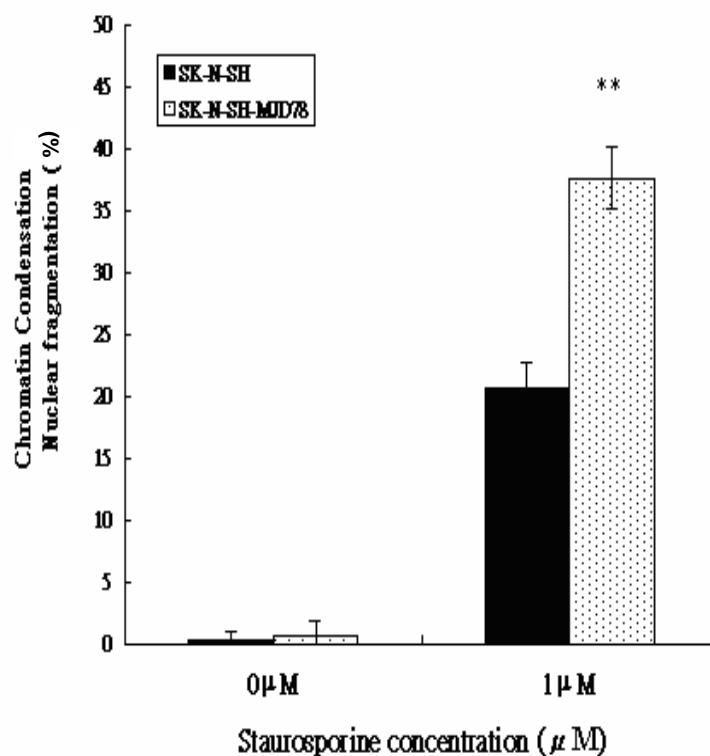


Fig. 1. (D) Quantitative assessment of apoptotic cells with or without staurosporine treatment. Nuclear DNA fragmentation of apoptotic cells was identified morphologically by nuclear dye DAPI fluorescent staining pattern of chromatin condensation. The number of the DAPI stained DNA fragmentation in 100 counted nuclei is called Apoptotic Index. Data were expressed as mean \pm SD from three separate experiments (** $P < 0.01$).

(A)

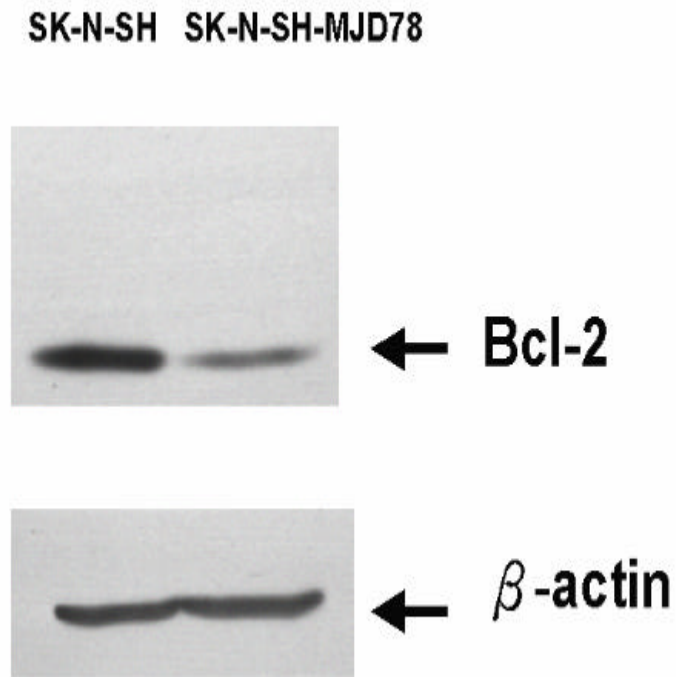


Fig. 2. (A) Bcl-2 levels in SK-N-SH and SK-N-SH-MJD78 cells. Proteins extracted from cells were loaded onto a 12% gel (30 μ g/well) for SDS-PAGE. The transferred blot was double labeled with Bcl-2 and β -actin monoclonal antibodies to show different levels of the protein expression in SK-N-SH and SK-N-SH-MJD78 cells.

(B)

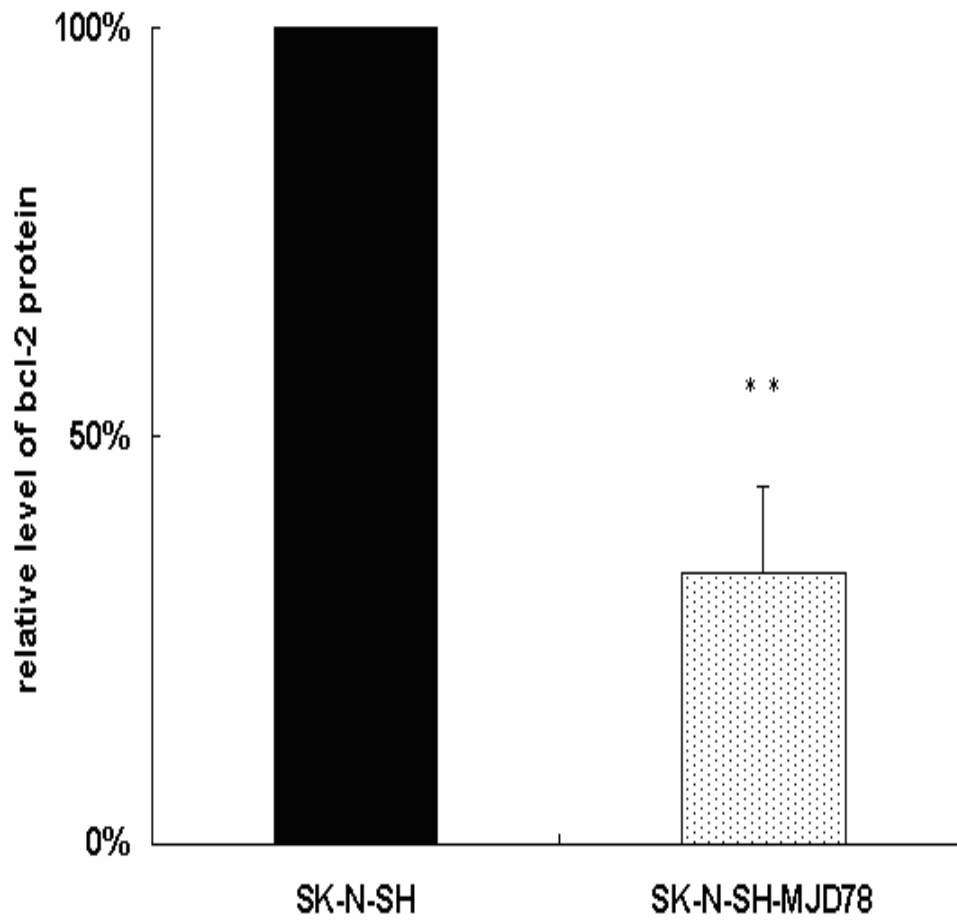
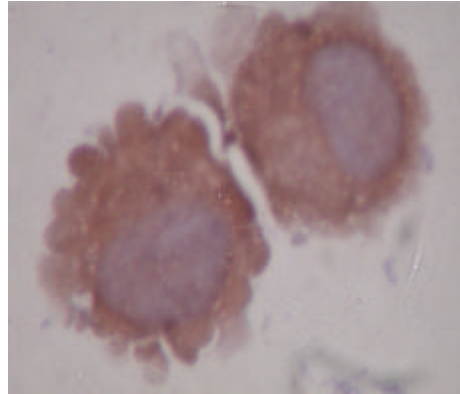


Fig. 2. (B) Quantitative assessment of Bcl-2 expression in SK-N-SH and SK-N-SH-MJD78 cells. The band intensity was assessed by an image analysis program (LAS-1000 plus). Compared to the level of an β -actin internal control, the mean relative levels of Bcl-2 protein in SK-N-SH and SK-N-SH-MJD78 cells were plotted with error bars representing standard deviations. $n = 4$, * * $P < 0.01$ compared with that of wild type.

(C)

SK-N-SH



SK-N-SH-MJD78

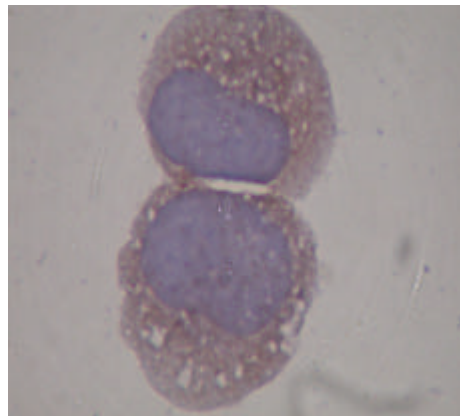


Fig. 2. (C) Immunocytochemical analysis of expressed Bcl-2. SK-N-SH and SK-N-SH-MJD78 cells were labeled with a monoclonal anti-Bcl-2 antibody. (Magnification: 1000X)

(D)

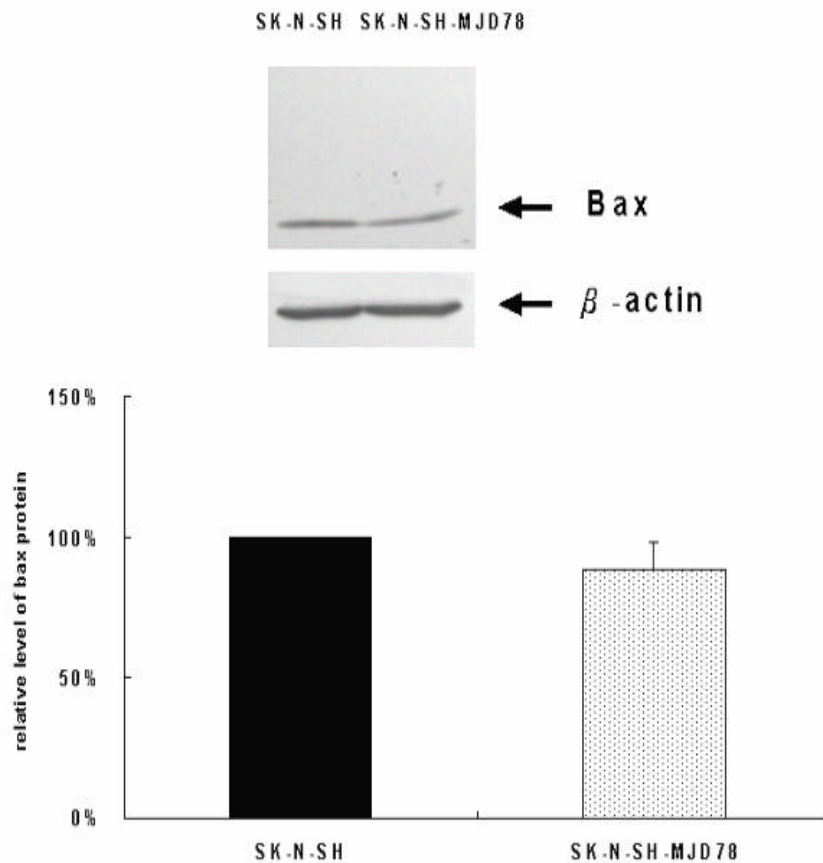


Fig. 2. (D) Bax protein levels in SK-N-SH and SK-N-SH MJD78 cells. The levels of Bax protein expression in SK-N-SH and SK-N-SH MJD78 cells were shown by a Western blot double labeled with Bax and β -actin monoclonal antibodies. Quantitative assessment of Bax expression in SK-N-SH and SK-N-SH-MJD78 cells. The band intensity was assessed by an image analysis program (LAS-1000 plus). Compared to the level of an β -actin internal control, the mean relative levels of Bad protein in SK-N-SH and SK-N-SH-MJD78 cells were plotted with error bars representing standard deviations ($n = 3$).

(E)

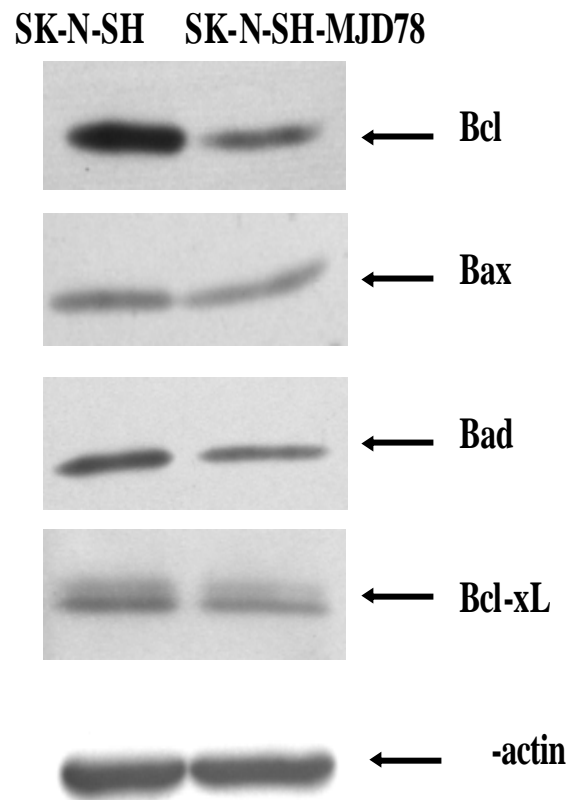


Fig. 2. (E) Western blot analysis with cell extracts of SK-N-SH and SK-N-SH-MJD78 cells. Proteins of Bcl-2 family were immunostained using specific antibodies against Bcl-2, Bax, Bad and Bcl-xL. Luminescent protein bands were generated using SuperSignal Substrate and visualized with Hyperfilm-ECL. Anti- β -actin antibody was used as an internal control.

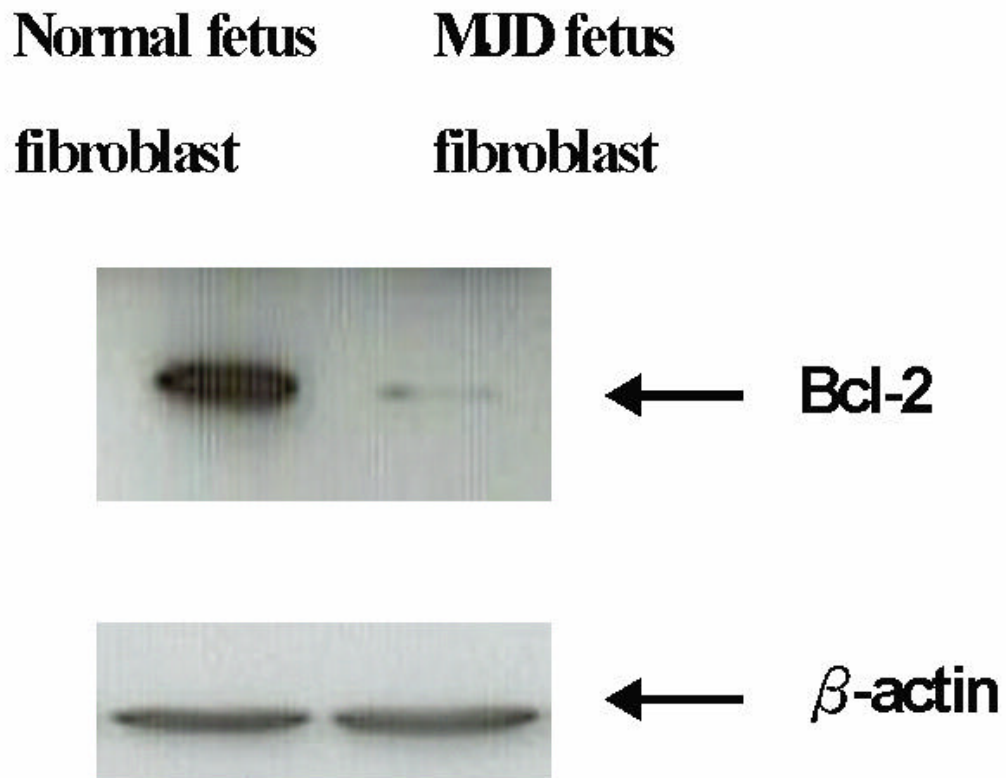


Fig. 3. Bcl-2 levels in fibroblast cells from a normal fetus and a MJD fetus. Western blot analysis was performed by using total protein (30 μ g/well) isolated from fibroblast cells. Monoclonal anti-Bcl-2 antibody was used in the blotting and anti- β -actin antibody was used as an internal control.

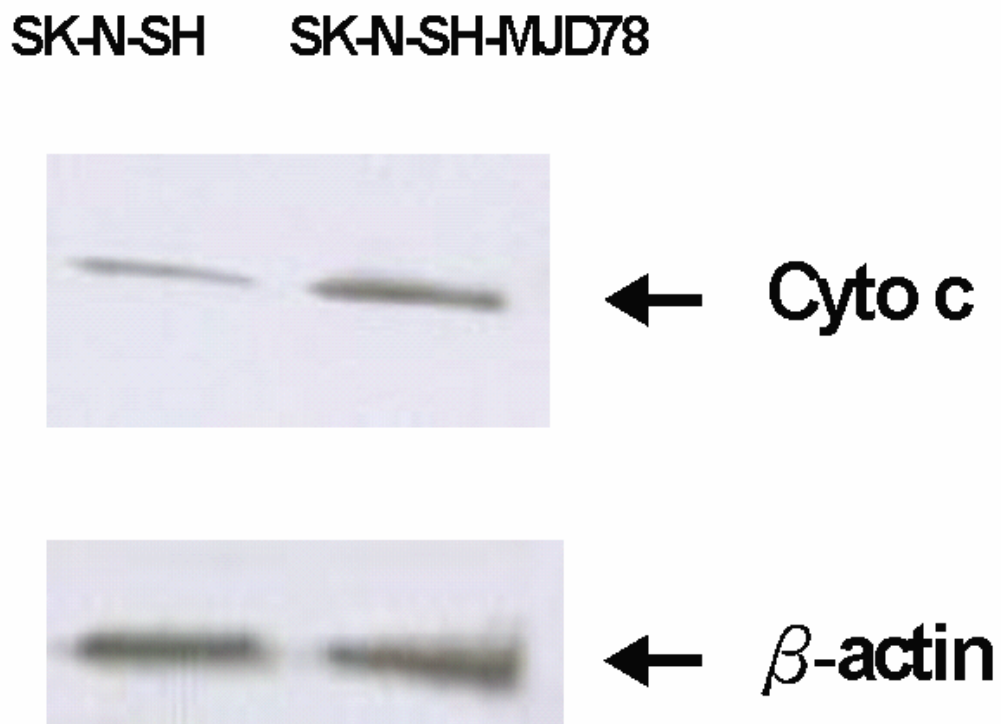


Fig. 4. Cytosolic cytochrome *c* levels in SK-N-SH and SK-N-SH MJD78 cells. Western blot analysis of the parental SK-N-SH cells and SK-N-SH-MJD78. Monoclonal anti-cytochrome *c* was used in the blotting. Anti- β -actin antibody was used as an internal control.

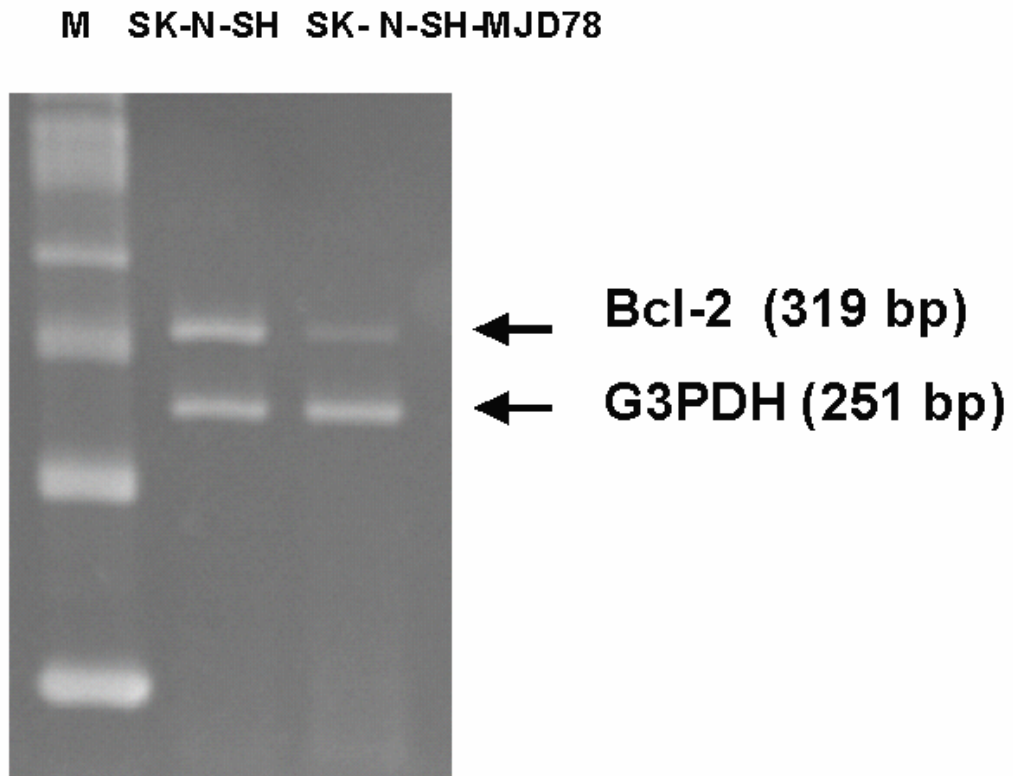


Fig. 5. Semi-quantitative RT-PCR of Bcl-2 gene expression. Total RNA from SK-N-SH and SK-N-SH-MJD78 were analyzed.

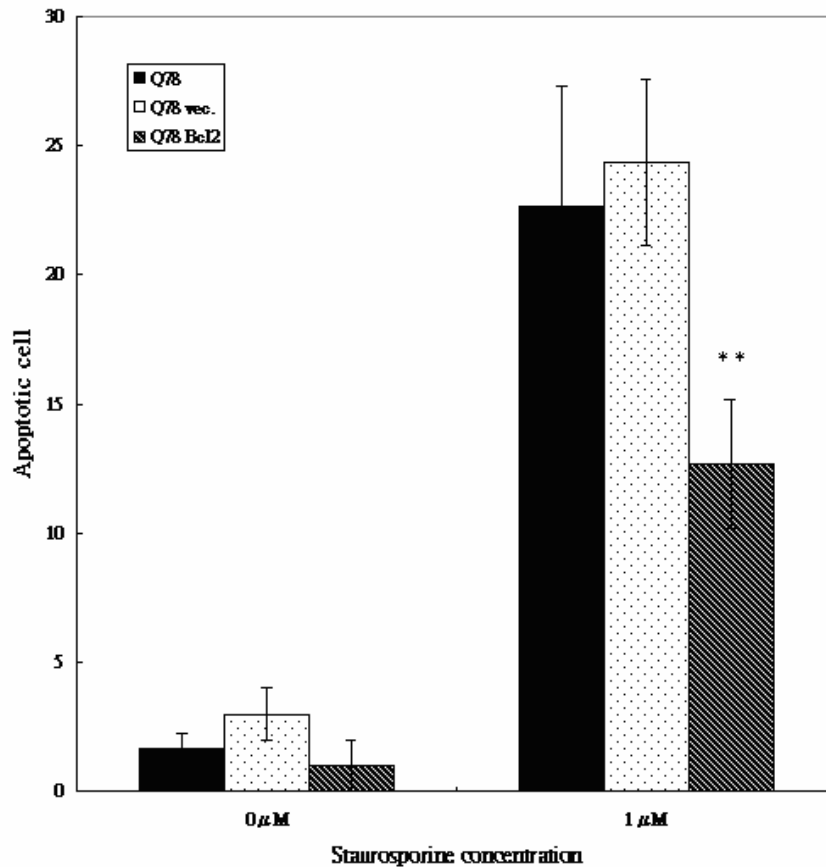


Fig. 6. Bcl-2 overexpression protects against poly (Q) toxicity. In SK-N-SH-MJD78 cells transfected with either pEGFP plus pcDNA3.1 vector or pEGFP plus pcDNA3-Bcl-2. Transfected cells were treated with 1 μ M STS for 24h, and reduced cell death as evidenced by nuclear fragmentation. Cells were analyzed 48h after transfection. The number of the DAPI stained DNA fragmentation in 300 counted nuclei of the transfected positive cells is called Apoptotic Index. Data were expressed as mean \pm SD from 3 different fields of two separate experiments. (** $P < 0.01$)

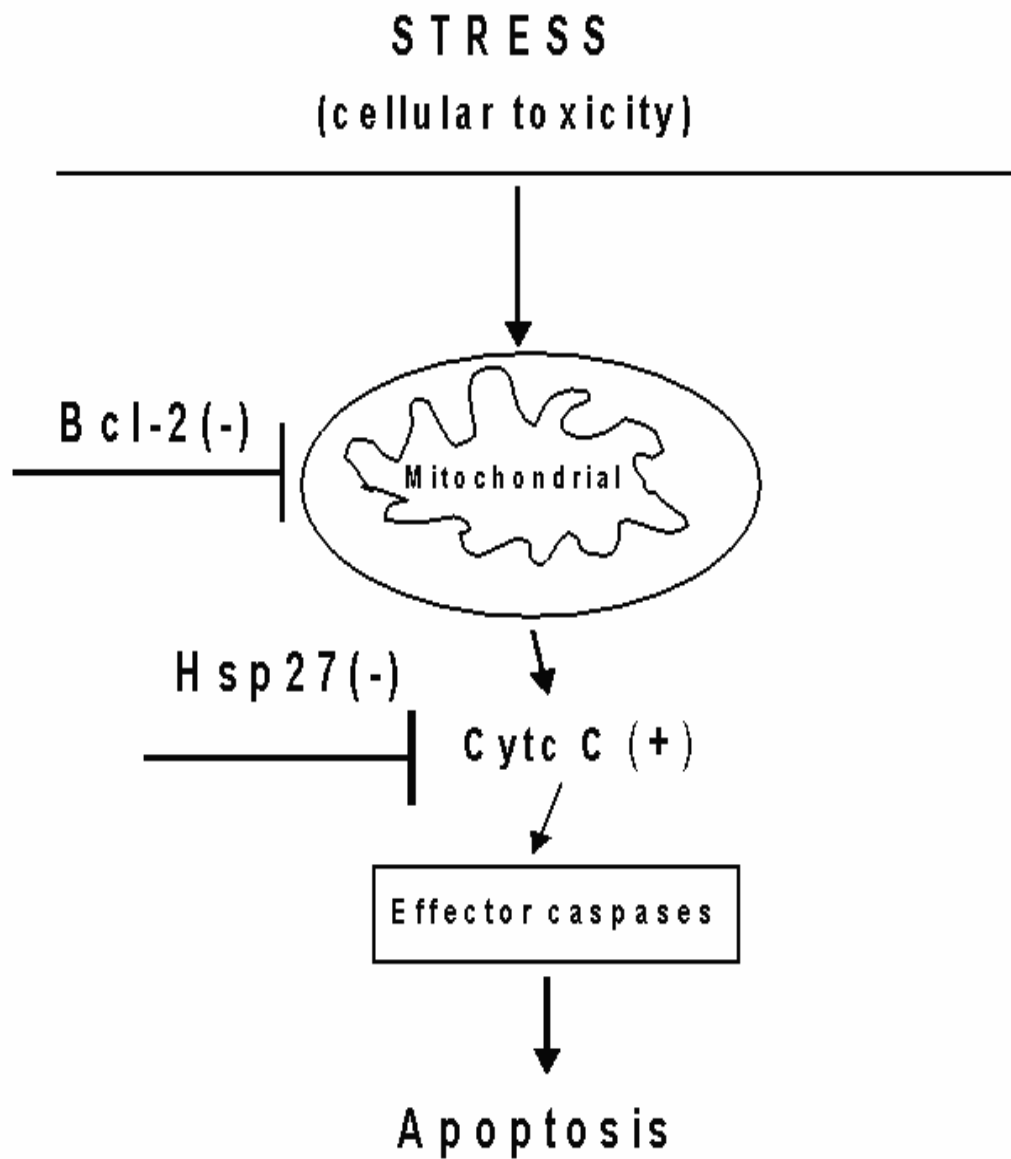


Fig. 7. Schematic representation of the role of classical apoptotic pathway in the pathogenesis of MJD disease. A hypothesis of ataxin-3 induced cell apoptosis pathway.

3-5 REFERENCES

1. Zoghbi HY and Orr HT. Glutamine repeats and neurodegeneration. *Annu. Rev. Neurosci.* 23 (2000) 217-247.
2. Alfen N, van, Sinke RJ, Zwarts MJ, et al. Intermediate CAG repeat lengths (53, 54) for MJD/SCA3 are associated with an abnormal phenotype. *Ann. Neurol.* 49 (2001) 805-807.
3. Maciel P, Costa MC, Ferro A, et al. Improvement in the molecular diagnosis of Machado-Joseph disease. *Arch. Neurol.* 58 (2001) 1821-1827.
4. Paulson HL and Fischbeck KH. Trinucleotide repeats in neurogenetic disorders. *Annu. Rev. Neurosci.* 19 (1996) 79-107.
5. Gutekunst CA, Li SH, Yi H, et al. Nuclear and neuropil aggregates in Huntington's disease: relationship to neuropathology. *J. Neurosci.* 19 (1999) 2522-2534.
6. Li F, Macfarlan T, Pittman RN, Chakravarti D. Ataxin-3 is a histone-binding protein with two independent transcriptional corepressor activities. *J. Biol. Chem.* 277 (2002) 45004-45012.
7. Paulson HL, Perez MK, Trottier Y, et al. Intranuclear inclusions of expanded polyglutamine protein in spinocerebellar ataxia type 3. *Neuron* 19 (1997) 333-344.
8. Yoshizawa T, Yamagishi Y, Koseki N, et al. Cell cycle arrest enhances the in

- vitro cellular toxicity of the truncated Machado-Joseph disease gene product with an expanded polyglutamine stretch. *Hum. Mol. Genet.* 9 (2000) 69-78.
9. Yoshizawa T, Yoshida H, Shoji S. Differential susceptibility of cultured cell lines to aggregate formation and cell death produced by the truncated Machado-Joseph disease gene product with an expanded polyglutamine stretch. *Brain Res. Bull* 56 (2001) 349-52.
 10. Yoshida H, Yoshizawa T, Shibasaki F, Shoji S, Kanazawa I. Chemical chaperones reduce aggregate formation and cell death caused by the truncated Machado-Joseph disease gene product with an expanded polyglutamine stretch. *Neurobiol. Dis.* 10 (2002) 88-99.
 11. Lombet A, Zujovic V, Kandouz M, et al. Resistance to induced apoptosis in the human neuroblastoma cell line SK-N-SH in relation to neuronal differentiation. Role of Bcl-2 protein family. *Eur. J. Biochem.* 268 (2001) 1352-1362.
 12. Fadeel B, Orrenius S, Zhivotovsky B. The most unkindest cut of all: on the multiple roles of mammalian caspases. *Leukemia* 14 (2000) 1514-1525.
 13. Blagosklonny MV. The dilemma of apoptosis in myelodysplasia and leukemia: a new promise of therapeutic intervention? *Leukemia* 14 (2000) 1502-1508.
 14. Nakagawa T, Zhu H, Morishima N, et al. Caspase-12 mediates endoplasmic-reticulum-specific apoptosis and cytotoxicity by amyloid-beta. *Nature* 403 (2000) 98-103.
 15. Solary E, Droin N, Bettaieb A, et al. Positive and negative regulation of

apoptotic pathways by cytotoxic agents in hematological malignancies.

Leukemia 14 (2000) 1833-1849.

16. Green DR and Reed JC. Mitochondria and apoptosis. *Science* 281 (1998) 1309-1312.
17. Davies AM. The Bcl-2 family of proteins, and the regulation of neuronal survival. *Trends Neurosci.* 18 (1995) 355-358.
18. Garcia I, Martinou I, Tsujimoto Y, Martinou JC. Prevention of programmed cell death of sympathetic neurons by the bcl-2 proto-oncogene. *Science* 258 (1992) 302-304.
19. Martinou JC, Dubois-Dauphin M, Staple JK, et al. Overexpression of BCL-2 in transgenic mice protects neurons from naturally occurring cell death and experimental ischemia. *Neuron* 13 (1994) 1017-1030.
20. Motoyama N, Wang F, Roth K A, et al. Massive cell death of immature hematopoietic cells and neurons in Bcl-x-deficient mice. *Science* 267 (1995) 1506-1510.
21. Oltvai ZN, Milliman CL, Korsmeyer SJ. Bcl-2 heterodimerizes in vivo with a conserved homolog, Bax, that accelerates programmed cell death. *Cell* 74 (1993) 609-619.
22. Saudou F, Finkbeiner S, Devys D, Greenberg ME. Huntingtin acts in the nucleus to induce apoptosis but death does not correlate with the formation of intranuclear inclusions. *Cell* 95 (1998) 55-66.

23. Ona VO, Li M, Vonsattel JP, et al. Friedlander RM. Inhibition of caspase-1 slows disease progression in a mouse model of Huntington's disease. *Nature* 399 (1999) 263-267.
24. Sawa A, Wiegand GW, Cooper J, et al. Increased apoptosis of Huntington disease lymphoblasts associated with repeat length-dependent mitochondrial depolarization. *Nat. Med.* 5 (1999) 1194-1198.
25. Wen FC, Li YH, Tsai HF, et al. Down-regulation of heat shock protein 27 in neuronal cells and non-neuronal cells expressing mutant ataxin-3. *FEBS Lett.* 546 (2003) 307-314.
26. Tsai HF, Liu CS, Chen GD, et al. Prenatal diagnosis of Machado-Joseph disease/Spinocerebellar Ataxia Type 3 in Taiwan: early detection of expanded ataxin-3. *J. Clin. Lab. Anal.* 17 (2003) 195-200.
27. Chen MC, Hsu TL, Luh TY and Hsieh SL. Overexpression of Bcl-2 Enhances LIGHT- and Interferon- γ -mediated Apoptosis in Hep3BT2 Cells. *J. Bio. Chem.* 275 (2000) 38794-38801.
28. Satyal SH, Schmidt E, Kitagawa K, et al. Polyglutamine aggregates alter protein folding homeostasis in *Caenorhabditis elegans*. *Proc. Natl. Acad. Sci. U S A.* 97 (2000) 5750-5755.
29. Reed JC. Bcl-2 and the regulation of programmed cell death. *J. Cell Biol.* 124 (1994) 1-6.
30. Evert BO, Wullner U, Schulz JB, et al. High level expression of expanded

- full-length ataxin-3 in vitro causes cell death and formation of intranuclear inclusions in neuronal cells. *Hum. Mol. Genet.* 7 (1999) 1169-76.
31. Kouroku Y, Fujita E, Jimbo A, et al. Polyglutamine aggregates stimulate ER stress signals and caspase-12 activation. *Hum. Mol. Genet.* 13 (2002) 1505-1515.
 32. Hockenbery D, Nunez G, Millman C, Schreiber RD, Korsmeyer SJ. Bcl-2 is an inner mitochondrial membrane protein that blocks programmed cell death. *Nature* 348 (1990) 334-336.
 33. Zhong LT, Sarafian R, Kane DJ, et al. Bcl-2 inhibits death of central neural cells induced by multiple agents. *Proc. Natl. Acad. Sci. USA.* 90 (1993) 4533-4537.
 34. Schmidt T, Lindenberg KS, Krebs A, et al. Protein surveillance machinery in brains with spinocerebellar ataxia type 3: redistribution and differential recruitment of 26S proteasome subunits and chaperones to neuronal intranuclear inclusions. *Ann. Neurol.* 51 (2002) 302-310.
 35. Warrick JM, Chan HY, Gray-Board GL, et al. Suppression of polyglutamine-mediated neurodegeneration in *Drosophila* by the molecular chaperone HSP70. *Nat. Genet.* 23 (1999) 425-428.
 36. Hsieh M, Tsai HF, Chang WH. HSP27 and cell death in Spinocerebellar Ataxia Type 3. (2004) *The Cerebellum*, in press.
 37. Evert BO, Vogt IR, Vieira-Saecker AM, et al. Gene expression profiling in ataxin-3 expressing cell lines reveals distinct effects of normal and mutant ataxin-3. *J. Neuropathol. Exp. Neurol.* 62 (2003) 1006-1018.

Chapter 4. Decreased expression of Hsp 27 and Hsp70 in transformed lymphoblastoid from patients with Spinocerebellar ataxia type 7 (SCA7)

ABSTRACT

Spinocerebellar ataxia type 7 (SCA7) is caused by an expansion of unstable CAG repeats within the coding region of the novel gene, ataxin-7, on chromosome 3. This disease is also associated with an accumulation of abnormal proteins, including expanded polyglutamine-containing proteins, molecular chaperones, and the ubiquitin-proteasome system. In this study, two SCA7 lymphoblastoid cell lines with 100 and 41 polyglutamine repeats were utilized to examine the effects of polyglutamine expansion on heat shock proteins. Interestingly, under basal conditions, western blot and immunocytochemical analysis showed a significant decrease of Hsp27 and Hsp70 protein expression in cells containing expanded ataxin-7, as compared with that of the normal LCL cells. However, the protein levels of Hsp60 and Hsp90 were not significantly altered in the mutant LCL cells. Therefore, by triggering the Heat Stress (HS) and assaying the expression of Hsp27 and Hsp70 under various recovery times, the heat shock response of the mutant cells was assessed and compared to that of cells without mutant ataxin-7. Our results demonstrated that even though the protein expression of Hsp27 and Hsp70 is defective, a normal heat shock response is present in lymphoblastoid cells expressing mutant ataxin-7. In addition, the results from proteasome inhibitor treatment indicated that the reduction of Hsp27 may not be due to the blockade of the proteasome

degradation pathway. Taken together, our results indicated that expanded ataxin-7 that leads to neurodegeneration significantly impaired the expression of Hsp27 and Hsp70 protein, which may be, at least in part, responsible for the toxicity of mutant ataxin-7 proteins and ultimately resulted in an increase of stress-induced cell death.

4-1 INTRODUCTION

SCA7 is classified as an autosomal dominant cerebellar ataxia type II (ADCA II), because affected patients display retinal and brain stem degeneration(1). The autosomal dominant cerebellar ataxias (ADCAs) are a heterogeneous group of disorders (2, 3) with variable onset and different clinical and neuropathological features, reflecting the degree of cerebellar and brain stem dysfunction.

Neuropathological examinations have certified the clinical picture, revealing marked atrophy of the cerebellar vermis, the inferior olivary nucleus, and the dentate nucleus (4). Neuronal loss and degenerative changes are consequently greatest in the Purkinje cell layer of the cerebellum and in the inferior olivary complex. A compelling feature of SCA7 is the genetic anticipation with an earlier age at onset and a more severe progression of disease in successive generations (1, 5). The causative mutation in SCA7 patients is an expansion of a CAG repeat within the 5' coding region, giving rise to an expanded polyglutamine stretch in the N-terminal portion of ataxin-7. In SCA7, a polymorphic CAG repeat with 4-35 repeats to 37 and over 300 repeats in the coding region of the *SCA7* gene (6). Ataxin-7 is a novel protein of unknown function of 892 amino acids residues, an isoelectric point of 9.87 and a predicted molecular mass of 95 kDa (7). The polyglutamine repeat disease group consists of at least nine

inherited neurodegenerative disorders, including spinal and bulbar muscular atrophy (SBMA), dentatorubral-pallidoluysian atrophy (DRPLA), Huntington's disease (HD), and six types of spinocerebellar ataxia type 1, 2, 3, 6, 7, and 17 (8, 9). These diseases are also associated with abnormal protein accumulations containing the disease protein, typically forming nuclear inclusions (NIs). NIs are also colocalized with many components of ubiquitin-proteasome, molecular chaperones, transcriptional regulators and other (Q)_n - containing proteins (10-14). Proteasomes are large multi-subunit protease complexes, which are localized in the nucleus and cytosol, and selectively degrade intracellular proteins (15). A vast majority of short-lived, normal proteins and misfolded, abnormal proteins are degraded by this system. Expanded polyglutamine tracts appeared to be more resistant to the degradation by the proteasome (16).

Aggregates in many (Q)_n disorders co-localize with ubiquitin, chaperones such as heat shock protein (Hsp) 70, Hsp40, Hsp90, HDJ-2 and various components of the proteasomes (17-24). Hsp have also been shown to suppress aggregate formation and cellular toxicity in a wide range of polyQ disease models (18, 25, 26). The main inducible HSPs in the nervous system are Hsp27 and Hsp70, which were shown to be neuroprotective. In particular, over-expression of Hsp70 chaperon could increase

neuronal survival upon neurotrophic factor or serum removal-induced apoptosis (27). Hsp70 functions as a major cellular protection molecule against protein aggregation (28) and is protective against a wide range of lethal stimuli. Overexpression of chaperones Hsp70, Hsp40, HDJ-2, and MRJ have all been shown to reduce aggregation, increase solubility, and reduce cell toxicity *in vitro* and in a *Drosophila* model (18, 23, 29). Altogether, these findings suggested that polyglutamine disease is associated with an abnormal protein conformation and the molecular chaperones may play a role in disease progression. It is possible that upregulated expressions of chaperone proteins may prevent misfolding and aggregation initiation at a point upstream of aggregate-mediated neurotoxicity.

Lymphoblasts have been known to express ataxin-7, and lymphoblasts from patients have been identified with expanded CAG repeats within the *SCA7* gene (30). To advance our understanding of polyglutamine neurodegeneration, we have generated a lymphoblastoid cell lines model for *SCA7*. In this study, both the patient and his father containing expressing ataxin-7 with 41 and 100 glutamines developed a neurological phenotype presenting as a gait ataxia. These results indicated that down-regulation of chaperone proteins occurs in human lymphoblastoid cell lines derived from human *SCA7*. These findings suggested that lymphoblastoid cell lines

may be of great value in gaining knowledge of cellular chaperone of ataxin-7. In this study, we showed here for the first time that the protein expression of Hsp27 and Hsp70 dramatically decreased in the presence of expanded ataxin-7. Our results suggested that the extent of polyglutamine-dependent protein aggregation and cellular toxicity may not be reduced due to the defects in Hsp27 and Hsp70.

4-2 MATERIALS AND METHODS

Reagents and antibodies:

All materials for cell culture were obtained from Gibco Life Technologies (Gaithersburg, MD). Reagents for western blot were obtained from Pierce (Rockford, USA). *N*-acetyl-leucyl-norleucinal (aLLN) was obtained from Sigma. For protease inhibition studies, cells were treated with 20 μ M aLLN. Mouse monoclonal antibodies against Hsp27, 60, 70 and 90 were from Lab Vision (Fremont, CA, USA). A mouse monoclonal antibody against β -actin and alkaline phosphatase-conjugated secondary antibodies were obtained from Sigma.

Preparation of lymphoblastoid cells:

Lymphoblastoid cells from two SCA7 affected patients with alleles containing 13 and 41, 16 and 100 CAG repeats, respectively, and normal control with 12 CAG repeats were established by Epstein-Barr virus transformation. The detail procedures were as described previously (31). All cell lines were cultured in RPMI-1640 medium and harvested with an amount of $1 \times 10^{7-8}$ cells. Lymphoblastoid cells were grown in RPMI-1640 (MEM; Gibco BRL) supplemented with 10% fetal bovin serum (FBS; Gibco BRL), 2 mM L-Glutamine, 1% PS (100 000U/L Penicillin G sodium, 100 mg/L Streptomycin sulfate). The medium was changed every 2 days and cells were

sub-cultivated weekly at a ratio of 1:2 and maintained at 37 °C in a humidified atmosphere with 5% CO₂.

PCR analysis:

For intergenerational repeat instability, DNA was isolated from lymphoblastoid cells by standard protocol (32). The SCA7 CAG repeat was PCR-amplified using primers 4U1024 and 4U716, as described previously (33). Briefly, all PCR reactions were performed as follows: in 20 µl reactions containing 10 mM Tris-HCl (pH 8.8), 1.5 mM MgCl₂, 50 mM KCl, 0.1% Triton X-100, 10% dimethylsulfoxide, 200 µM dNTPs, 80 ng of each primer, and 3 units of Taq DNA polymerase with 100 ng DNA being the template. After a pre-denaturation step at 94°C for 5 mins, 35 cycles of 96°C for 40 s, 57°C for 30 s, and 72°C for 1.5 min were performed followed by a final extension at 72°C for 10 mins. To determine the size range of CAG repeat expansion, the PCR products were analyzed on 3% agarose gels in parallel with the 100 bp marker and visualized by ethidium bromide (EB). Allele size was determined by comparison with the 100 bp marker, assuming that the variation in the size of the product occurs within the repetitive CAG stretch.

Preparation of cell lysates for SDS-PAGE:

Cells were washed twice with phosphate buffered saline (PBS, pH 7.2), resuspended in 500 µl of lysis buffer (5% glycerol, 1 mM sodium EDTA, 1 mM

sodium EGTA, 1 mM dithiothreitol, 40 µg/ml leupeptin, 40 µg/ml aprotinin, 20 µg/ml pepstain, 1 mM PMSF, 0.5 % Triton X-100, 1× PBS) and then incubated on ice for 15 min. Resultant cell lysate was centrifuged at 16,000 rpm for 20 min at 4 °C. Supernatant was collected, and Bio-Rad protein assay reagent was used to determine the protein concentrations.

Western blotting:

In brief, cell lysates containing 20 µg of protein were loaded onto 12 % sodium dodecyl sulfate (SDS)-polyacrylamide gels. Resolved proteins were electrophoretically transferred onto 0.2 µm nitrocellulose membranes. After blocking the membrane with 5% nonfat milk in NaCl/Pi/0.1% Tween 20 for 1 h at room temperature, the antibody-binding reactions were performed in the same buffer supplemented with 1% nonfat milk at 4 °C overnight for monoclonal anti-Hsp27, 60, 70, 90 or Bcl-2 (1:500) and at room temperature for 1 h for secondary antibodies coupled to horseradish peroxidase (HRP)-conjugated anti-goat IgG. Prestained high molecular weight markers (Rainbow colored protein molecular weight markers from Amersham) were included in this study. Signals were visualized with the enhanced chemiluminescence.

Heat-shock treatment:

LCL cells were suspended at 1×10^6 cells per ml in closed polyethylene tubes

(15 ml), heat shocked by incubating in a water bath for 1 h at 42 °C and allowed to recover for 0, 5, 10, 15, 20 h at 37 °C for the maximum production of HSPs.

Immunocytochemistry:

Cells, collected using cytopsin, were fixed with 4% paraformaldehyde in 0.1 M phosphate-buffered saline (pH 7.4) for 10 min. They were treated with 0.3% H₂O₂ in 100% EtOH for 10 min to eliminate endogenous peroxidase and incubated with 10% normal goat serum (ABC kit, Zymed, South San Francisco, CA) at 37 °C for 1 h.

Cells were incubated with Hsp27 or Hsp70 antibodies (1:100) in 10% normal goat serum overnight at 4 °C. After the primary incubation, cells were treated with biotinylated secondary antibodies (DAKO kit) for 1 h at 37 °C, followed by an incubation with a streptavidin peroxidase conjugate (DAKO kit) for 1 h at 37°C.

Immunolabels were visualized with 3,3-diaminobenzidine staining kit (Zymed) and counter-stained with Meyer's Hematoxylin.

Isolation of total RNA and semi-quantitative RT-PCR:

Total RNA was extracted from cells using Trizol reagent (Life Technologies, USA). For each sample, 3 µg of RNA was reverse-transcribed into cDNA in a final volume of 20 µl with 50 pmol oligo d(T) and 50 units MMLv reverse transcriptase (Perkin Elmer, USA) for 15 min at 42° C. The mRNA for bcl-2 and G3PDH were

measured by semi-quantitative RT-PCR. The primers used were: Hsp70 upstream 5' - TGACCTTCGACATCGATGC-3', Hsp70 downstream 5' -TGTTGAAGGCGTAGG ACTCC-3'; G3PDH upstream 5' -CCATGTTCGTCATGGGTGTGAACCA-3', downstream ' -GCCAGTAGAGGCAGGGATGATGTTC-3'. Hsp27-F 5' - TGGATGTCAACCACTTCGC -3', Hsp27-R 5' - TGGTGATCTCGTTGGACTGC -3', β -actin A 5' - GGCGGCACCACCATGTACCCT -3', β -actin B 5' - AGGGGCCGG ACTCGT CAT ACT - 3'. PCR reaction was performed in a final volume of 25 μ l with 5 μ l from the RT reaction for cDNA amplification. The PCR mixture contained 20 pmol each of upstream and down stream primers and 1 unit Taq polymerase (Promega, USA). PCR conditions of Hsp70 were as the followings: an initial denature for 5 min at 95 °C, followed by 30 s at 95°C, 1 min at 57.5°C, 30 s at 72°C, for 28 cycles. Another one PCR conditions of Hsp27 were as the followings: an initial denature for 5 min at 95 °C, followed by 30 s at 95°C, 1 min at 60°C, 30 s at 72°C, for 28 cycles. A sample without RNA was included in each experiment of RT-PCR as a negative control. Ethidium bromide-stained PCR products were separated on 3% agarose gels, visualized and quantified using a LAS-1000 plus imaging analyzer (Fujifilm, Japan). The sizes of the amplified products were 219 bp and 251 bp for Hsp70 and G3PDH, or 246 bp and 200 bp for Hsp27 and β -actin, respectively. In order to compare the amplified products semi-quantitatively,

quantitation of the signals was performed using a densitometric scanner. The use of G3PDH provided good control of the bias caused by possible degradation of the mRNA. We had earlier confirmed that after 28 amplification cycles, the RT-PCR reactions were in a linear range and not at a plateau (data not shown).

4-3 RESULTS

Determination of CAG triplet repeat expansion in SCA7 and control lymphoblastoid cell lines

PCR of the CAG triplet repeat region of the SCA7 gene was first performed in lymphoblastoid cells from two SCA7 patients, and a normal unaffected healthy individual, to illustrate effective determination of CAG repeats by PCR. Our results indicated that PCR products resolve relatively clear signals on 3% agarose gels (Fig.1). PCR of genomic DNA from the normal lymphoblastoid cell line generated bands of about 300 bp-320 bp suggesting the presence of two alleles of the SCA7 gene (lane 1). PCR of genomic DNA from the juvenile SCA7 lymphoblastoid cell line produced a band of 320 bp and another larger band of about 650 bp (lane 3). It was noted that the upper PCR band from juvenile and paternal SCA7 lymphoblastoid cell lines contained around 40 and 100 CAG repeats, demonstrating the successful expansion of the mutant SCA7 gene in the cell lines. In the following studies, lymphoblastoid cell lines (LCLs) from these two SCA7 patients and one normal individual were used for comparison.

Full-length ataxin-7 in juvenile SCA7, adult onset SCA7, and control lymphoblastoid cell lines

Next, we examined the expression of normal and mutant full-length ataxin-7 in these three lymphoblastoid cell lines. Western blot analysis was performed, using 8% SDS-PAGE gels, with antibodies that recognize the NH₂- and COOH-domains of ataxin-7 (Fig. 2). The upper band of the doublet in the juvenile SCA7 lymphoblastoid was consistent with the presence of the expanded ataxin-7 with 100 polyglutamine repeats (lane 3). The lower band was consistent with full-length ataxin-7 of normal polyQ repeat length of 10 repeats. In the normal lymphoblastoid cell line, the single band of full-length ataxin-7 would correspond to the normal number of polyQ repeats of 10 and 12 repeats for the two normal alleles in this cell line. The results revealed normal protein expression from both the mutant and normal alleles in the corresponding cell lines.

Expression of Bcl-2 protein under normal conditions

Because the expression of Bcl-2 is decreased in the presence of mutant ataxin-3, as mentioned in the previous chapter, we compared the protein expression of Bcl-2 in the presence and absence of mutant ataxin-7 in the SCA7 cellular model. However,

our results demonstrated that the expression of Bcl-2 did not differ significantly between cells with and without expanded ataxin-7 (Fig. 3A and 3B).

Protein expression of Hsp27 and Hsp70 dramatically decreased in the presence of expanded ataxin-7

Given the polyglutamine disease is associated with abnormal protein conformation, the molecular chaperones may play a role in disease progression. In order to understand whether there is any defect in the chaperone expression, Western blot analysis was performed first using monoclonal antibody against Hsp27 or Hsp70. A representative Western blot was shown in Figure 4A. The results demonstrated that the protein levels of Hsp27 and Hsp70 in the SCA7 patient's lymphoblastoid cells significantly decreased (lane 2 and lane 3 of Fig. 4A) compared with that of the normal LCL cells (lane 1 of Fig. 4A). This observation was further confirmed by immunocytochemical staining using mouse monoclonal antibody against Hsp27 and Hsp70. As shown in Figure 4B, significant positive staining was observed in the normal LCL cells (Fig. 4B) compared with very weak staining in cells containing expanded ataxin-7 (Fig. 4B). Furthermore, we compared the expression of other heat shock proteins in our cellular model to understand whether the reduction of Hsp70 was due to a common effect on heat shock response. By contrast, other stress

associated heat shock proteins, namely Hsp60 and Hsp90, remained unaffected in mutant ataxin-7 cells. These results indicated that the altered protein expression of Hsp27 and Hsp70 was specific in the cellular model. We next determined whether this reduction in Hsp27 and Hsp70 was due to transcriptional repression of HSP27 and HSP 70 gene. Semiquantitative RT-PCR revealed similar expressing of Hsp27 transcripts in cells with and without mutant ataxin-7 (Fig. 4C). However, a significant decrease in Hsp70 mRNA levels was observed in cells expressing mutant ataxin-7 as compared to that of the normal cells (Fig. 4D), with G3PDH as the internal control (Fig. 4D). This observation suggested that the down-regulation of Hsp70 protein expression is due to the defects at the transcriptional level. But the down-regulation of Hsp27 protein expression is not due to the transcriptional dysfunction.

Increased of Hsp27 but not Hsp70 in cells treated with proteasome inhibitors

aLLN is a synthetic aldehydic tripeptide that can, *in vitro*, inhibit the activity of Ca²⁺-dependent neutral cysteine proteases. aLLN can also inhibit lysosomal proteases, including cathepsin L, cathepsin B, and calpain D (Hiwasa et al., 1990). The aLLN has been shown to inhibit proteasome activity (Rock, L. K. 1994, Ward, C. L 1995, Lowe, J. 1995). To see whether proteasomes are involved in the processing of Hsp27,

we used proteasome inhibitors to block the possible degradation pathway. Cells that stably express the SCA7 gene were treated for 24 h with the peptide aldehyde aLLN (20 μ M), and the Hsp content was analyzed in Western immunoblots developed with the Hsp27 or Hsp70. Our results showed that the aLLN proteasome inhibitor induced a large increase in the total amount of Hsp70 (Figure 5). However, the Hsp27 was not prominent even after 24 h treatment with aLLN (Figure 5). Our results indicated that the degradation pathway of Hsp27 may not go through the proteasome degradation.

Heat shock induces the expression of Hsp27 and 70

To understand whether the heat shock response is altered in the presence of mutant ataxin-7, the normal control and SCA7 affected patient's lymphoblastoid cells were treated with a modest increase in growth temperature. After subjecting these cells to heat treatment at various temperatures, we found that 42 °C for 1h is the optimal condition (data not show). The untreated or treated cells under this condition were then allowed to recover from the heat shock for 0, 5, 10, 15, 20 h and the protein expression of Hsps 27, 70 or 60 were verified by Western blot analysis. To make sure the equal loading of 30 μ g protein in all the samples, β -actin controls were included. These results showed a dramatic increase in the protein levels of Hsp27 and Hsp70 but not Hsp60 in the heat-treated cultures recovery (5 h) in normal control and mutant ataxin-7 cells (lane 3 of Fig. 6). However, the expression levels of Hsp27 and Hsp70

in the presence of mutant ataxin-7 showed a slight decrease at after 10 h, but the expressions of Hsps 27, 70 (but not 60) were still higher than the basal levels at 0 h (Figure 6). These results suggest that the optimal conditions of heat shock chosen for the study are sufficient to induce the expression of the Hsps 27, 70 (but not 60) in SCA7 affected patient's lymphoblastoid cells and their expression was still maintained above basal levels in control and mutant ataxin-7 cells during the recovery period of 5-20 h.

4-4 DISCUSSION

In the present study, we have generated lymphoblastoid cell lines containing normal and mutant human ataxin-7, derived from the normal individual and SCA7 patients. A patient with subclinical spinocerebellar ataxia type 7 (SCA7) was detected with a borderline mutation of 41 CAG repeats and his son with juvenile-onset SCA7 was detected with about 100 repeats (5). In an effort to determine whether the expression of expanded ataxin-7 leads to the altered gene expression in the chaperone proteins, which have been identified to reduce the intranuclear inclusions observed in SCAs (18, 25, 26, 28), Western blot analysis was performed to examine the expression levels of heat shock proteins, such as Hsp27, Hsp60, Hsp70 or Hsp90. The results from Western blot and immunocytochemistry demonstrated a significant reduction of Hsp27 and Hsp70 in lymphoblastoid cell lines with expanded ataxin-7, but the levels of Hsp60 and Hsp90 were unaltered. Our results were consistent to that previously reported to reveal a decrease in Hsp70 in the retina of R6/1 and R7E SCA7 mouse models (38). It is now well established that the appearance of many unfolded polypeptides in the cytosol or nucleus was the common intracellular signal for induction of the heat shock proteins at high temperatures and in other stressful conditions (39, 40). Because the reduction of Hsp27 and Hsp70, we wonder whether

the heat shock response is intact in the presence of mutant ataxin-7. Cells with or without ataxin-7 were treated with a brief heat stress followed by different recovery periods (0, 5, 10, 15 and 20 h), then the cells were harvested and Western blot analysis was performed to assess the heat shock response. Two major heat-shock proteins, Hsp27 and Hsp70, were examined and a parallel induction of expression of Hsp27 and Hsp70 was observed, but not Hsp60 (Fig 6). Our results suggested that the cells expressing mutant ataxin-7 still remain normal response to the heat shock stress, as compared to that of the wild type cells. There may be a significant link between the heat-shock response and mechanisms of poly Q folding and degradation. Many of the major heat-shock proteins function as molecular chaperones involved in the folding, assembly, and/or degradation of aggregated, misfolded, or damaged proteins (41). In agreement with the abovementioned observation, it was recently reported that there was a decrease in the levels of several heat shock proteins (Hdj1, Hdj2 and Hsp70), which correlates with phenotype progression in a R6/2 mice model of Huntington's disease, and that pharmacological induction of chaperones significantly delayed aggregates formation in an organotypic slice culture assay (42). The polyglutamine disease is associated with an abnormal protein conformation; the molecular chaperones may play a role in disease progression. Therefore, decreased levels of Hsp27 and Hsp70 in the cellular milieu could lead to the failure of many cellular

processes.

In addition, it is worthy to note that the reduced Hsp27 expression was not due to transcriptional dysregulation, as indicated through semiquantitative RT-PCR (Fig 4C). On the other hand, the down-regulation of Hsp70 expression was due to the defect at the transcriptional level (Fig 4D). Our results indicated that the gene expression defects of Hsp27 and Hsp70 in the presence of mutant ataxin-7 may be due to different control levels, either at the level of translation or transcription. It is known that reduced Hsp70 gene expression in differentiated PC12 cells could increase the sensitivity of cells to pathophysiological stress (43). Further studies will be required to address the mechanism underlying the reduced mRNA level of Hsp70 in the disease model. Recent investigations have demonstrated that proteasomal inhibition can lead to a heat-shock response, expression of chaperones, and thermotolerance (44), suggesting that accumulation of misfolded proteins initiates the stress response. Our results demonstrated an accumulation of Hsp70, but not Hsp27, was observed after the treatment of proteasom inhibitors (Fig. 5). The failure of aLLN-induced Hsp27 indicated that the degradation of Hsp27 may not go through the proteasome degradation pathway in lymphoblastoid cells. Our results are consistent to previously reported that aLLN proteasome inhibitor selectively increased HSP70 levels without

affecting Hsp25, Hsp27, Hsp60, Hsp86, Hsp90, Hsp104, or Bip in HepG2 (45). In our study, the aLLN-induced increase in Hsp70 synthesis may be result from increased transcription of the *hsp72* gene via activation of HSF1 and inhibition of proteasome degradation as previously reported (45).

Various evidences have suggested that in neurodegenerative diseases such as HD, AD and PD, the most prominent feature is protein aggregates within neurons or extracellular protein deposits. It immediately became obvious that there is a potential involvement of the cellular machinery preventing the accumulation of misfolded proteins, and therefore the role of molecular chaperones in neurodegeneration became very important (46). Furthermore, the neurotoxicity of abnormal poly Q proteins was suppressed by Hsp70 (47), the up-regulation of which under stress assists re-folding of misfolded protein (28). Overexpression of Hsp27 was also demonstrated to prevent cellular polyglutamine toxicity and suppressed the increase levels of cellular reactive oxygen species (ROS) caused by huntingtin (26). In a previous study, we have demonstrated that the endogenous Hsp27 expression is decreased in an early disease model of spinocerebellar ataxia type 3 (48). However, the mechanisms of how HSP27 involved in the pathogenesis of polyglutamine disease remained unclear.

In conclusion, we have shown that the reduction of Hsp 27 and Hsp70 proteins

was observed in the SCA7 lymphoblastoid cells, which may lead to misfolded protein accumulation and cell-toxicity stress. Aggregation of poly Q could enhance these stresses, by recruiting chaperones and proteasomal components (18). The degree to which the HS response may protect against cellular damage in specific diseases has been studied only to a very limited extent. In this study, we demonstrated that the normal heat shock response is intact in the presence of mutant ataxin-7. Therefore, it is potentially very important to further analyze the pharmacological induction of Hsp proteins, which might be an effective approach to reduce cell injury and inhibit disease progression.

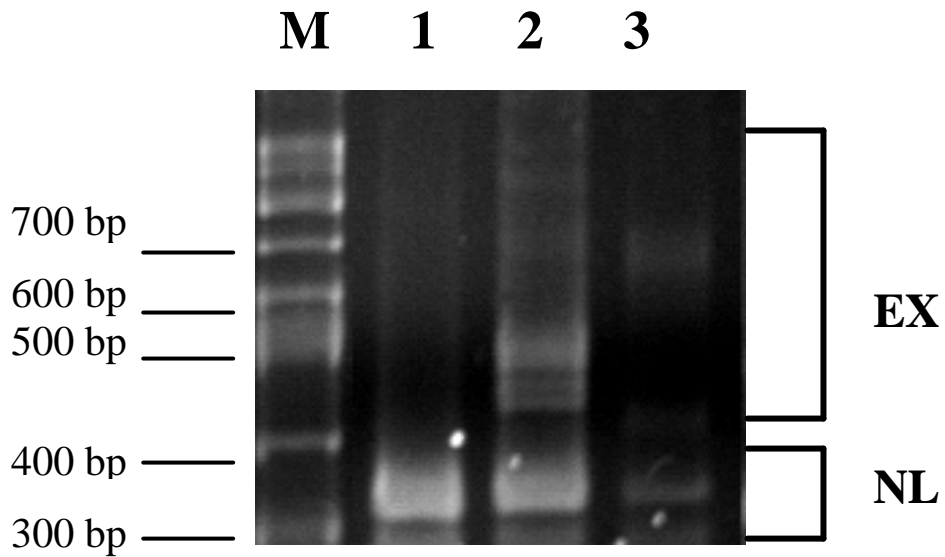


Figure 1: Detection of the CAG expansion in the ataxin-7 gene on a 3% agarose gel. PCR analysis of DNAs. One DNA fragment with lower molecular weight below 300 bp was observed a non-related human wild type control (lane 1), while the expanded mutant alleles were found from the cells derived from the father, and son (lanes 2 and 3) with moderated mosaic DNA fragments and range around 400-650 bp. EX, expanded allele; NL, normal allele.

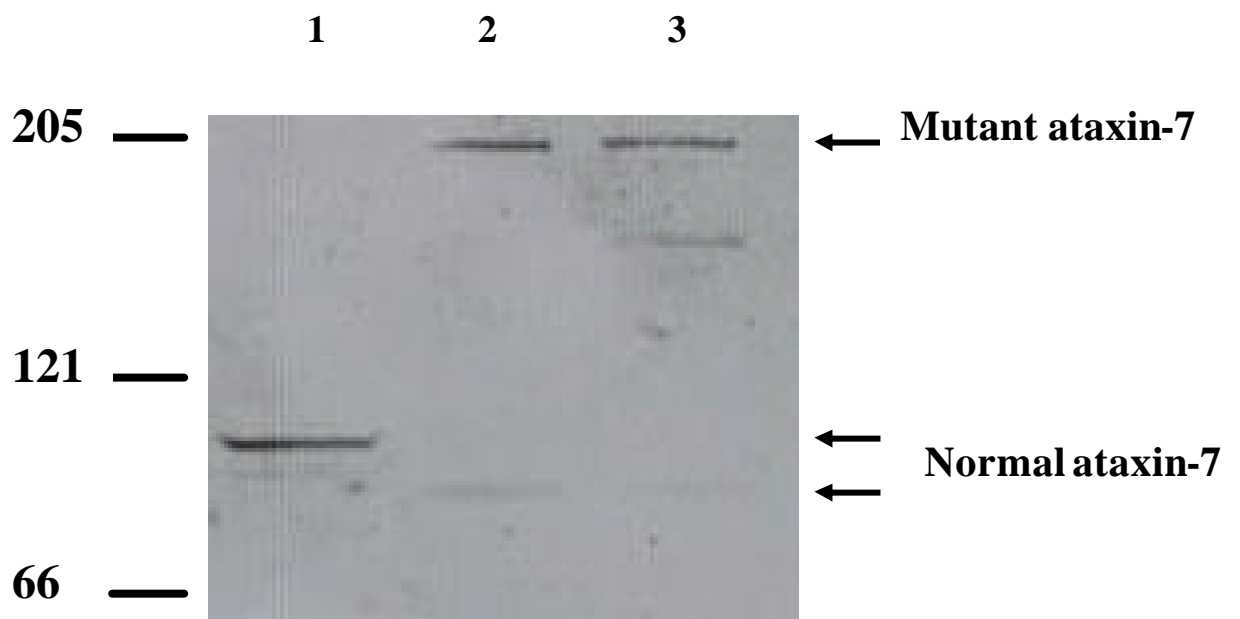


Figure 2: Western blot analysis of ataxin-7 in lymphoblastoid cells from SCA7 affected and normal individuals. Normal lymphoblastoid cells (lane 1) and lymphoblastoid cells from two affected individuals (lanes 2 and 3) were cultured in complete medium. Western blot was probed with polyclonal anti-ataxin-7 antibodies.

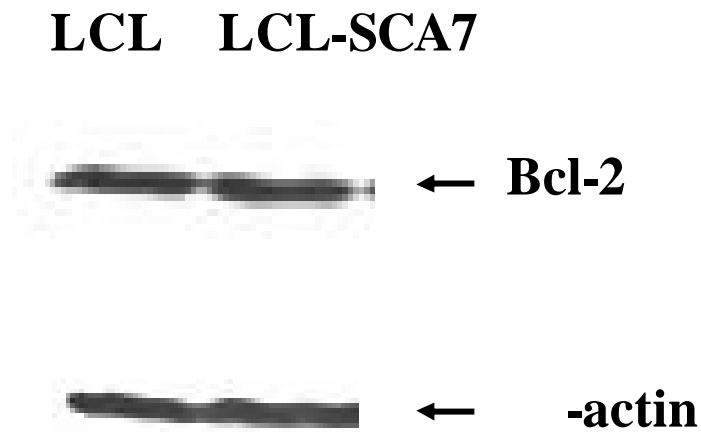


Figure 3: (A) Bcl-2 levels in lymphoblastoid cells from SCA7 affected and normal individuals. Proteins extracted from cells were loaded onto a 12% gel (30 μ g/well) for SDS-PAGE. The transferred blot was double labeled with Bcl-2 and β -actin monoclonal antibodies to show different levels of the protein expression in lymphoblastoid cells from SCA7 affected and normal individuals.

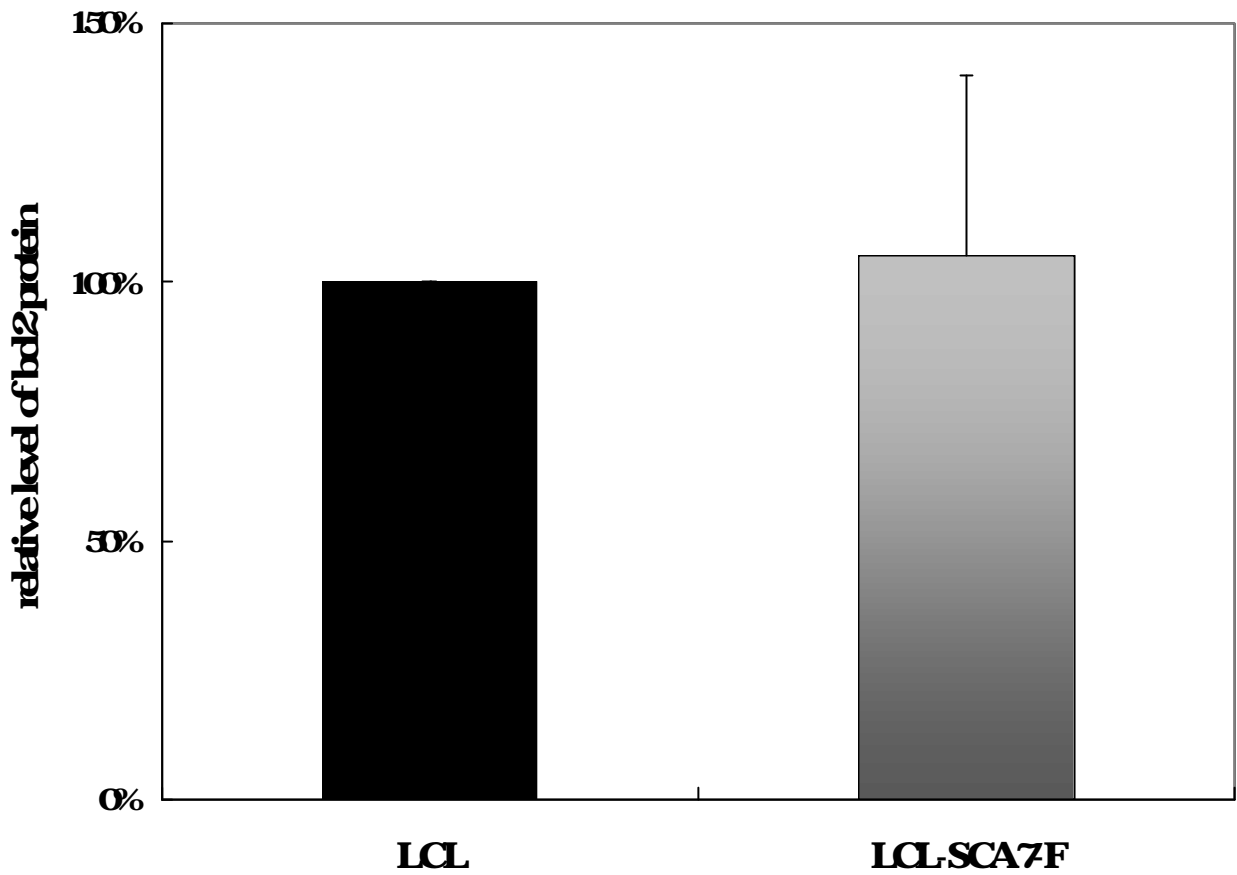


Figure 3: (B) Quantitative assessment of Bcl-2 expression in lymphoblastoid cells from SCA7 affected and normal individuals. The band intensity was assessed by an image analysis program (LAS-1000 plus). Compared to the level of an β -actin internal control, the mean relative levels of Bcl-2 protein in lymphoblastoid cells from SCA7 affected and normal individuals were plotted with error bars representing standard deviations. $n = 3$.

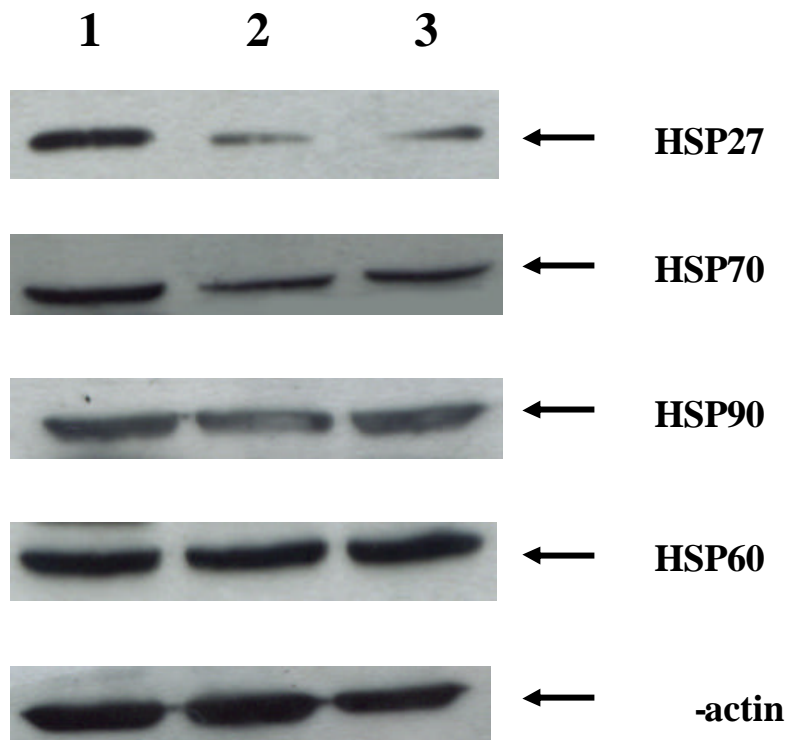


Figure 4: (A) Western blot analysis of HSP27, HSP60, HSP 70 and HSP90 in lymphoblastoid cells from SCA7 affected and normal individuals. Normal lymphoblastoid cells (lane 1) and lymphoblastoid cells from two affect individuals (lanes 2 and 3) were cultured in complete medium. Cell lysates were electrophoresed, Western blotted and probed with anti-HSP27, anti-HSP60, anti-Hsp70 and anti-Hsp90 antibody together with anti- -actin antibody as an internal control.

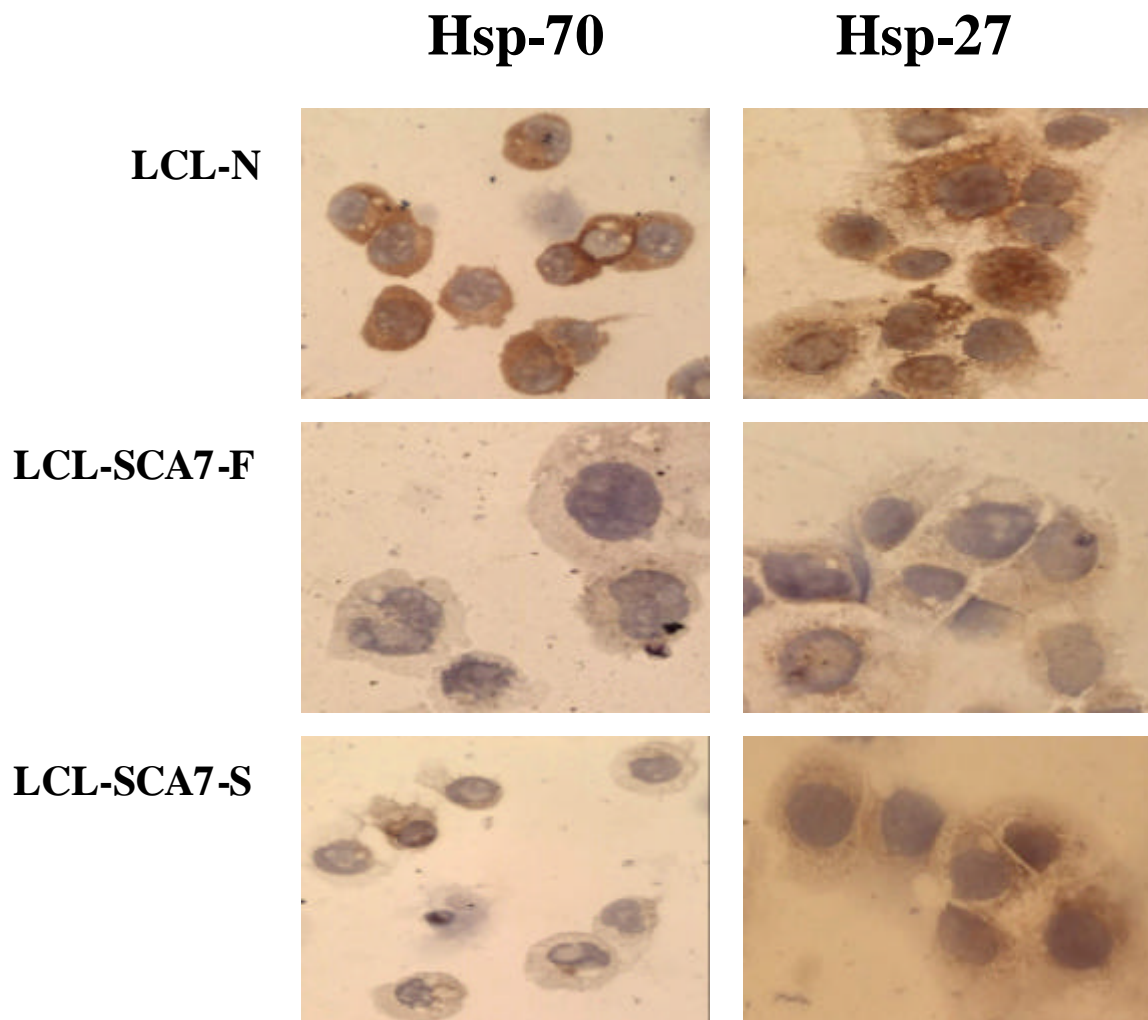


Figure 4: (B) Immunocytochemical analysis of expressed HSP27 and HSP70. lymphoblastoid cells were collected using cytopsin and labeled with monoclonal anti-HSP27 and HSP70 antibodies. (Magnification: 400X)

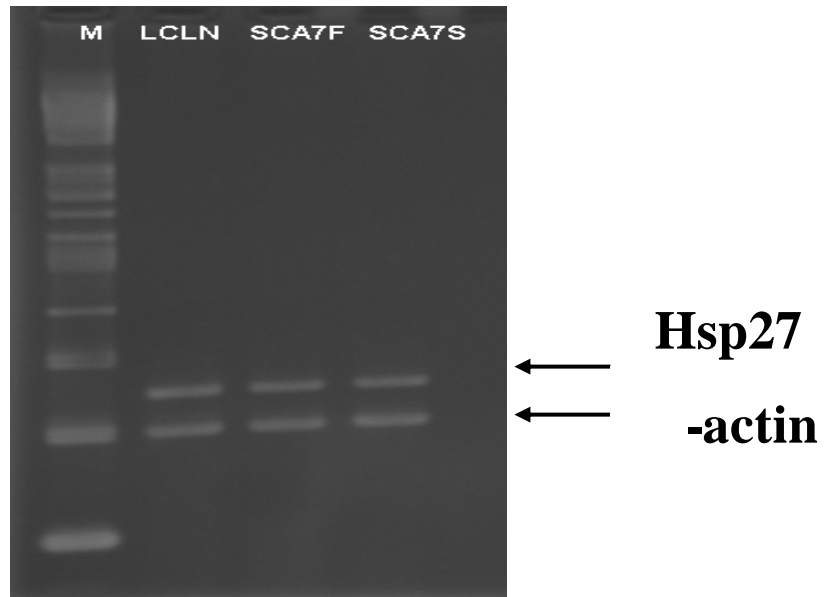


Figure 4: (C) Semi-quantitative RT-PCR of Hsp27 gene expression with β -actin gene as an internal control.

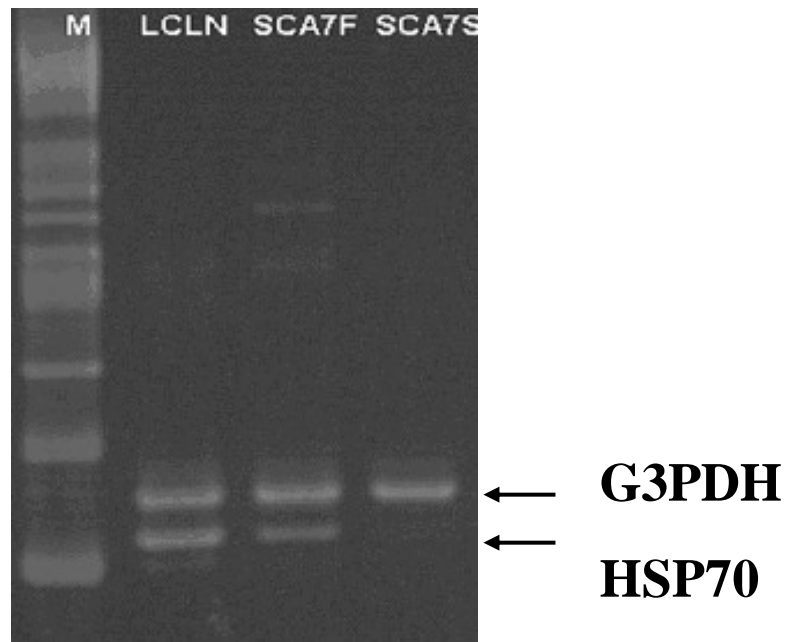


Figure 4: (D) Semi-quantitative RT-PCR of Hsp70 gene expression with G3PDH gene as an internal control. Total RNA from SCA7 affected and normal individual lymphoblastoid cells were analyzed.

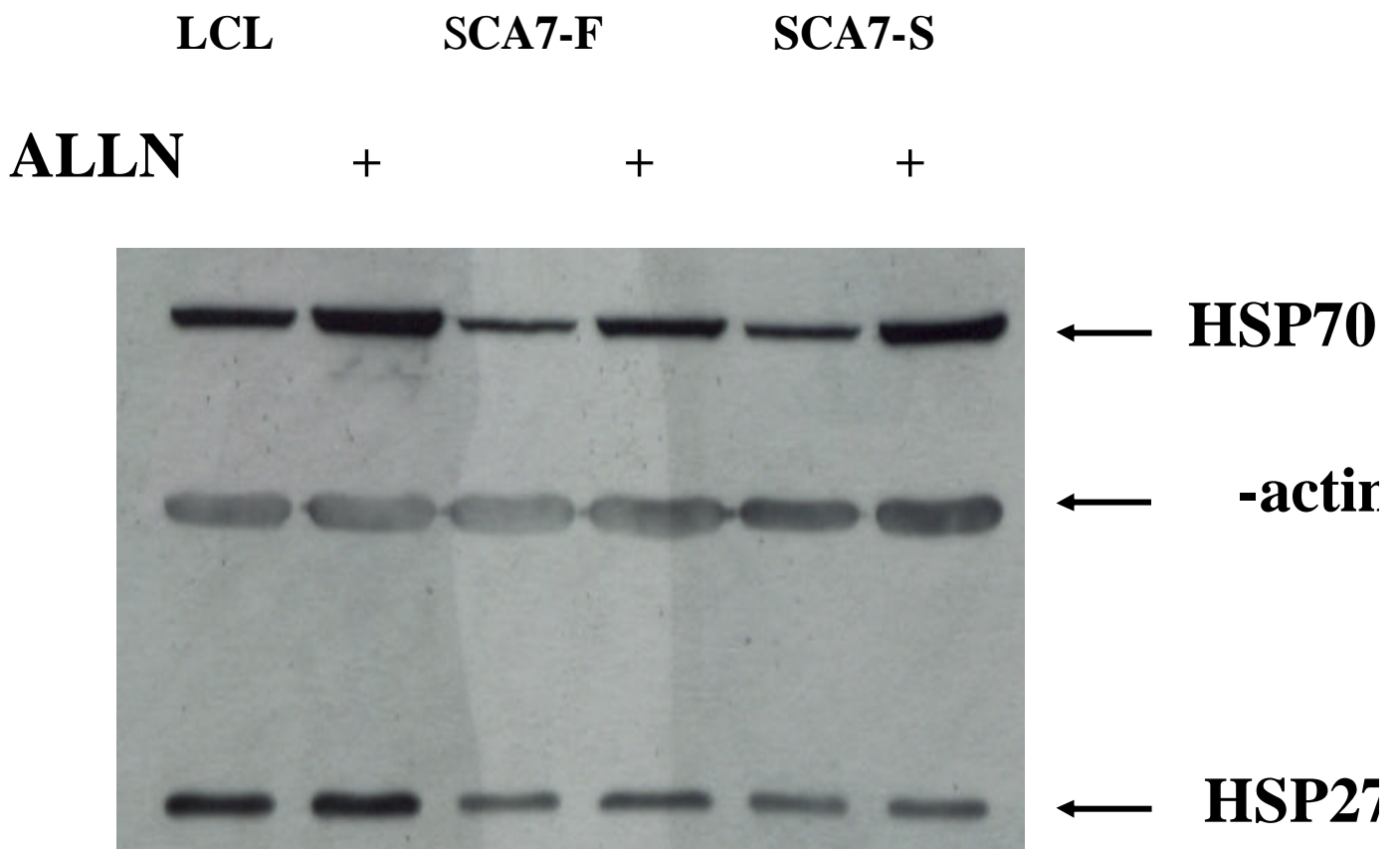


Figure 5: Effect of aLLN on heat shock protein in lymphoblastoid cells from SCA7 affected and normal individuals.

LCL

No HS	HS recovery time (h)				
	0	5	10	15	20

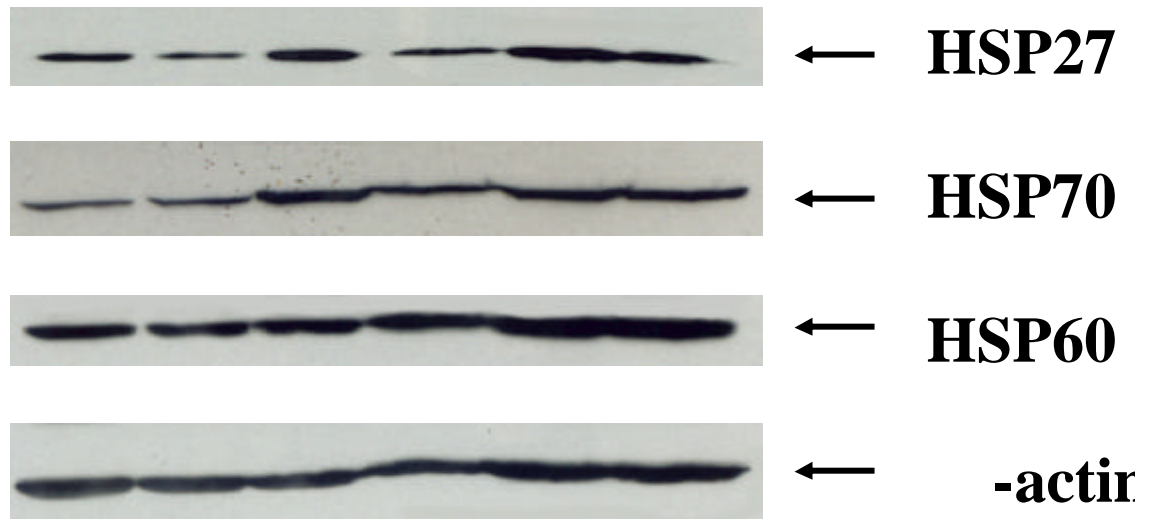


Figure 6: (A) Western blot analysis of Hsp27, Hsp60, Hsp 70 in heat shocked normal lymphoblastoid cells were heat shocked for 1 h at 42 °C and allowed to recover for 0 h (lane 1), 5 (lane 2), 10 (lane 3), 15 (lane 4), 20 h (lane 5) at 37 °C for the maximum production of HSPs.

CL-SCA7

No	HS recovery time (h)				
HS	0	5	10	15	20

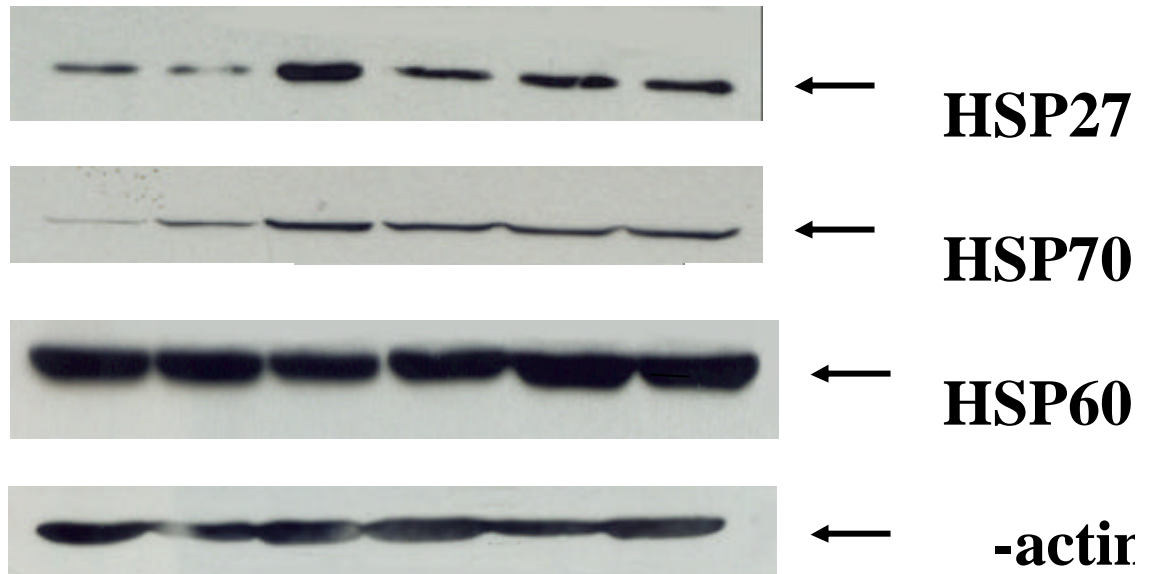


Figure 6: (B) Western blot analysis of Hsp27, Hsp60, Hsp 70 in heat shocked lymphoblastoid cells from SCA7 lymphoblastoid cells were heat shocked for 1 h at 42 and allowed to recover for 0 (lane 2), 5 (lane 3), 10 (lane 4), 15 (lane 5), 20 h (lane 6) at 37 for the maximum production of HSPs.

4-5 REFERENCE

1. Enevoldson TP, Sanders MD, Harding AE. Autosomal dominant cerebellar ataxia with pigmentary macular dystrophy. A clinical and genetic study of eight families. *Brain* 117 (1994) 445-460.
2. Harding AE. The clinical features and classification of the late onset autosomal dominant cerebellar ataxias. *Brain* 105 (1982) 1–28.
3. Harding AE. Clinical features and classification of inherited ataxias. *Adv Neurol* 61 (1993) 1–14.
4. Weiner LP, Konigsmark BW, Stoll Jr J, Magladery JW. Hereditary olivopontocerebellar atrophy with retinal degeneration. Report of a family through six generations. *Arch Neurol* 16 (1967) 364-376.
5. Hsieh M, Lin SJ, Chen JF, et al. Identification of the spinocerebellar ataxia type 7 mutation in Taiwan: application of PCR-based Southern blot. *J. Neurology* 247 (2000) 623-629.
6. Stevanin G, Durr A and Brice A. Clinical and molecular advances in autosomal dominant cerebellar ataxias: from genotype to phenotype and physiopathology. *Eur. J. Hum.Genet.* 8 (2000) 4-18.

7. Del-Favero J, Krols L, Michalik A, et al. Molecular genetic analysis of autosomal dominant cerebellar ataxia with retinal degeneration (ADCA type II) caused by CAG triplet repeat expansion. *Hum. Mol. Genet.* 7 (1998) 177-186.
8. Zoghbi HY and Orr HT. Glutamine repeats and neurodegeneration. *Annu. Rev. Neurosci.* 23 (2000) 217-247.
9. Nakamura K, Jeong SY, Uchihara T, et al. SCA17, a novel autosomal dominant cerebellar ataxia caused by an expanded polyglutamine in TATA-binding protein. *Hum. Mol. Genet.* 10 (2001) 1441-1448.
10. Paulson HL, Perez MK, Trotter Y, et al. Intranuclear inclusions of expanded polyglutamine protein in spinocerebellar ataxia type 3. *Neuron* 19 (1997) 333-344.
11. Cooper JK, Schilling G, Peters MF, et al. Truncated N-terminal fragments of huntingtin with expanded glutamine repeats form nuclear and cytoplasmic aggregates in cell culture. *Hum. Mol. Genet.* 7 (1998) 783-790.
12. Li SH and Li XJ. Aggregation of N-terminal huntingtin is dependent on the length of its glutamine repeats. *Hum. Mol. Genet.* 7 (1998) 777-782.
13. Martindale D, Hackman A, Wieczorek A, et al. Length of huntingtin and its polyglutamine tract influences localization and frequency of intracellular aggregates. *Nat. Genet.* 18 (1998) 150-154.

14. Zander C, Takahashi J, El Hachimi KH, et al. Similarities between spinocerebellar ataxia type 7 (SCA7) cell models and human brain: proteins recruited in inclusions and activation of caspase-3. *Hum. Mol. Genet.* 10 (2001) 2569-2579.
15. Kornitzer D and Ciechanover A. Modes of regulation of ubiquitin-mediated protein degradation. *J. Cell Physiol.* 182 (2000) 1–11.
16. Ding Q, Lewis JJ, Strum KM, et al. Polyglutamine expansion, protein aggregation, proteasome activity, and neural survival. *J. Biol. Chem.* 277 (2002) 13935–13942
17. Kalchman MA, Graham RK, Xia G, et al. Huntingtin is ubiquitinated and interacts with a specific ubiquitin-conjugating enzyme. *J. Biol. Chem.* 271 (1996) 19385-19394.
18. Cummings CJ, Mancini MA, Antalffy B, et al. Chaperone suppression of aggregation and altered subcellular proteasome localization imply protein misfolding in SCA1. *Nat. Genet.* 19 (1998) 148-154.
19. Chai Y, Koppenhafer SL, Bonini NM and Paulson HL. Analysis of the role of heat shock protein (Hsp) molecular chaperones in polyglutamine disease. *J. Neurosci.* 19 (1999) 10338–10347.
20. Chai YH, Koppenhafer SL, Shoemaker SJ, Perez MK, Paulson HL. Evidence for proteasome involvement in polyglutamine disease: localization to nuclear

inclusions in SCA3/MJD and suppression of polyglutamine aggregation in vitro. *Hum. Mol. Genet.* 8 (1999) 673-682.

21. Stenoiën DL, Cummings CJ, Adams HP, et al. Polyglutamine-expanded androgen receptors form aggregates that sequester heat shock proteins, proteasome components and SRC-1, and are suppressed by the HDJ-2 chaperone. *Hum. Mol. Genet.* 8 (1999) 731-741.
22. Waelter S, Boeddrich A, Lurz R, et al. Accumulation of mutant huntingtin fragments in aggresome-like inclusion bodies as a result of insufficient protein degradation. *Mol. Biol. Cell.* 12 (2001) 1393-1407.
23. Bailey CK, Andriola IF, Kampinga HH, Merry DE. Molecular chaperones enhance the degradation of expanded polyglutamine repeat androgen receptor in a cellular model of spinal and bulbar muscular atrophy. *Hum. Mol. Genet.* 11. (2002) 515-523.
24. Schmidt T, Lindenberg KS, Krebs A, et al. Protein surveillance machinery in brains with spinocerebellar ataxia type 3: redistribution and differential recruitment of 26S proteasome subunits and chaperones to neuronal intranuclear inclusions. *Ann. Neurol.* 51. (2002) 302-310.
25. Warrick JM, Chan HY, Gray-Board GL, Chai Y, Paulson HL and Bonini NM. Suppression of polyglutamine-mediated neurodegeneration in *Drosophila* by the molecular chaperone HSP70. *Nat. Genet.* 23 (1999) 425–428.

26. Wyttenbach A, Carmichael J, Swartz J, et al. Effects of heat shock, heat shock protein 40 (HDJ-2), and proteasome inhibition on protein aggregation in cellular models of Huntington's disease. *Proc. Natl. Acad. Sci. USA.* 97 (2000) 2898-2903.
27. Wagstaff MJ, Collaco-Moraes Y, Smith J, et al. Protection of neuronal cells from apoptosis by Hsp27 delivered with a herpes simplex virus-based vector. *J. Biol. Chem.* 274 (1999) 5061-5069.
28. Glover JR and Lindquist S. HSP104, HSP70, and HSP40: a novel chaperone system that rescues previously aggregated proteins. *Cell* 94 (1998) 73-82.
29. Chuang JZ, Zhou H, Zhu M, Li SH, Li XJ, Sung CH. Characterization of a brain-enriched chaperone, MRJ, that inhibits Huntingtin aggregation and toxicity independently. *J. Biol. Chem.* 277 (2002) 19831-19838.
30. Trottier Y, Lutz Y, Stevanin G, et al. Polyglutamine expansion as a pathological epitope in Huntington's disease and four dominant cerebellar ataxias. *Nature* 378. (1995) 403-406.
31. Neitzel H. A routine method for the establishment of permanent growing lymphoblastoid cell lines. *Hum. Genet.* 73 (1986) 320-326.
32. Sambrook J, Fritsch EF and Maniatis T. *Molecular Cloning: a Laboratory Manual.* (1989) Cold Spring Harbor Laboratory Press, Plainview, NY.

33. David G, Abbas N, Stevanin G, et al. Cloning of the SCA7 gene reveals a highly unstable CAG repeat expansion. *Nat. Genet.* 17 (1997) 65-70.
34. Hiwasa T, Sanada T, Sakiyama S. Cysteine proteinase inhibitors and ras gene products share the same biological activities including transforming activity toward NIH3T3 mouse fibroblasts and the differentiation-inducing activity toward PC12 rat pheochromocytoma cells. *Carcinogenesis* 11 (1990) 75-80.
35. Rock LK, Gramm C, Rothstein L, et al. Inhibitors of the proteasome block the degradation of most cell proteins and the generation of peptides presented on MHC class I molecules. *Cell* 78 (1994) 761-771.
36. Ward CL, Omura S, Kopito RR. Degradation of CFTR by the ubiquitin-proteasome pathway. *Cell* 83. (1995) 121-127.
37. Lowe J, Stock D, Jap B, et al. Crystal structure of the 20S proteasome from the archaeon *T. acidophilum* at 3.4 Å resolution. *Science* 268. (1995) 533-539.
38. Merienne K, Helmlinger D, Perkin GR, Devys D, Trottier Y. Polyglutamine expansion induces a protein-damaging stress connecting heat shock protein 70 to the JNK pathway. *J. Biol. Chem.* 278 (2003) 16957-16967.
39. Goff SA and Goldberg AL. Production of abnormal proteins in *E. coli* stimulates transcription of *lon* and other heat shock genes. *Cell* 41 (1985) 587-595.
40. Ananthan J, Goldberg AL, Voellmy R. Abnormal proteins serve as eukaryotic

stress signals and trigger the activation of heat shock genes. *Science* 232 (1986) 522-524.

41. Hayes SA and Dice JF. Roles of molecular chaperones in protein degradation. *J. Cell. Biol.* 132 (1996) 255–258.
42. Hay DG, Sathasivam K, Tobaben S, et al. Progressive decrease in chaperone protein levels in a mouse model of Huntington's disease and induction of stress proteins as a therapeutic approach. *Hum. Mol. Genet.* 13 (2004) 1389-1405.
43. Hatayama T, Takahashi H and Yamagishi N. Reduced induction of HSP70 in PC12 cells during neuronal differentiation. *J Biochem (Tokyo).* 122 (1997) 904-910.
44. Bush KT, Goldberg AL and Nigam SK. Proteasome inhibition leads to a heat-shock response, induction of endoplasmic reticulum chaperones, and thermotolerance. *J. Biol. Chem.* 272 (1997) 9086–9092.
45. Zhou M, Wu X, Ginsberg HN. Evidence that a rapidly turning over protein, normally degraded by proteasomes, regulates hsp72 gene transcription in HepG2 cells. *J. Biol. Chem.* 271 (1996) 24769-24775.
46. Muchowski PJ. Protein misfolding, amyloid formation, and neurodegeneration: a critical role for molecular chaperones? *Neuron* 35 (2002) 9-12.
47. Warrick JM, Chan HY, Gray-Board GL, et al. Suppression of

polyglutamine-mediated neurodegeneration in *Drosophila* by the molecular chaperone HSP70. *Nat. Genet.* 23 (1999) 425-428.

48. Wen FC, Li YH, Tsai HF, et al. Down-regulation of heat shock protein 27 in neuronal cells and non-neuronal cells expressing mutant ataxin-3. *FEBS Lett.* 546 (2003) 307-314.